DESIGN AND ANALYSIS OF LLC RESONANT CONVERTER FOR EV BATTERY CHARGING

A DISSERTATION

SUBMITTED IN PARTIAL FULFILLMENT OF THE RQUIREMENTS

FOR THE AWARD OF THE DEGREE

OF

MASTER OF TECHNOLOGY
IN
POWER ELECTRONICS AND SYSTEMS

Submitted by:

SHREYAS

2K21/PES/15

Under the supervision of

Dr. MAYANK KUMAR

DEPARTMENT OF ELECTRICAL ENGINEERING
DELHI TECHNOLOGICAL UNIVERSITY
(Formerly Delhi College of Engineering)
Bawana Road, Delhi-110042

MAY 2023

DEPARTMENT OF ELECTRICAL ENGINEERING
DELHI TECHNOLOGICAL UNIVERSITY
(Formerly Delhi College of Engineering)
Bawana Road, Delhi-110042

CANDIDATE'S DECLARATION

I Shreyas, Roll No. 2K21/PES/15 student of MTech (Power Electronicsand Systems), hereby declare that the project Dissertation titled "**Design and Analysis of LLC resonant converter for Electric Vehicle Battery Charging**" which is submitted by me to the Department of Electrical Engineering, Delhi Technological university, Delhi in partial fulfilment of the requirement for the award of the degree of Master of Technology, is original and not copied from any source without proper citation. This work has not previously formed the basis for the award of any Degree, Diploma Associateship, Fellowship or other similar title or recognition.

Place: Delhi **Shreyas**

Date: **(2K21/PES/15)**

DEPARTMENT OF ELECTRICAL ENGINEERING
DELHI TECHNOLOGICAL UNIVERSITY
(Formerly Delhi College of Engineering)
Bawana Road, Delhi-110042

CERTIFICATE

I hereby certify that the project Dissertation titled "**Design and Analysis of LLC resonant converter for Electric Vehicle Battery Charging**" which is submitted by Shreyas, Roll No. 2K21/PES/15, Department of Electrical Engineering, Delhi Technological University,Delhi in partial fulfilment of the requirement for the award of the degree of Master of Technology, is a record of the project work carried out by the student under my supervision. To the best of my knowledge this work has not been submitted in part or full for any Degree or Diploma to this University or elsewhere.

Place: Delhi

Date:

Dr. Mayank Kumar

SUPERVISOR

DEPARTMENT OF ELECTRICAL ENGINEERING
DELHI TECHNOLOGICAL UNIVERSITY
(Formerly Delhi College of Engineering)
Bawana Road, Delhi-110042

ACKNOWLEDGEMENT

I would like to express my gratitude towards all the people who have contributed their precious time and effort to help me without whom it would not have been possible for me to understand and complete the project. I would like to thank Dr. Mayank Kumar, DTU Delhi, Department of Electrical Engineering, my Project Supervisor, for supporting, motivating and encouraging me throughout the period of this work. His readiness for consultation at all times, his educative comments, his concern and assistance even with practical things have been invaluable.

Besides my supervisor, I would like to thank all the PhD scholars of EVRT LAB for helping me wherever required and provided me continuous motivation during my research.

Finally, I must express my very profound gratitude to my parents, seniors and to my friends for providing me with unfailing support and continuous encouragement throughout the research work.

Date:

Shreyas
MTech (Power Electronics & Systems)
Roll No. 2K21/PES/15

Abstract

The rechargeable batteries are changing the way of designing EVs. As the batteries are dc operated that always require dc-dc converter for controlling the stages of power conversion. Developing countries are replacing fuel driven vehicles with traditional, less expensive EVs which are driven by lead acid and lithium-ion batteries.

In order to achieve wide input range, minimal switching losses, and stable performance designing of resonant converters are required. This paper suggests effective methodology of battery charging using resonant converter. Resonant power converters have become quite popular recently in applications requiring solid-state transformers, solar PV fed EV (EV) charging infrastructures, etc.

Internal combustion (IC) engines have been the only type of engines used in international transportation networks for a very long period. Diesel, gasoline serve as the primary sources of energy for the vehicle engine in conventional transportation propulsion systems. Due to the hazardous CO_2 emissions emitted during combustion, the usage of such fuels results in health issues.

As a result, recent research and attention have focused heavily on electric and hybrid vehicles (HEV). It is done in order to reduce the hazardous gases emitted during the combustion of these fuels and pave the way to a clean and energy-efficient transportation system. In order to fulfil the requirement of power in the EV transportation, rechargeable batteries are essential in hybrid and electric automobiles.

TABLE OF CONTENTS

LIST OF FIGURES

LIST OF ABBREVIATION

S. No.	Abbreviated Name	Full Name
1.	EV	EV
2.	ICE	Internal Combustion Engine
3.	BEV	Battery EV
4.	G2V	Grid to Vehicle
5.	V2G	Vehicle to Grid
6.	V2L	Vehicle to Load
7.	PHEV	Plug-in Hybrid EV
8.	OBC	On-Board Charger
9.	NGV	Natural Gas Vehicle
10.	DCFC	Direct Current Fast Charging
11.	ZVS	Zero Voltage Switching
12.	ZCS	Zero Current Switching
13.	DAB	Dual Active Bridge
14.	ISOP	Input Series Output Parallel
15.	CC	Constant Current
16.	CV	Constant Voltage
17.	PI	Proportional Integrator
18.	LPF	Low Pass Filter
19.	PWM	Pulse Width Modulation
20.	SoC	State of Charge
21.	THD	Total Harmonics Distortion
22.	VSC	Voltage Source Converter
23.	UPF	Unity Power Factor

LIST OF SYMBOLS

S. No.	Symbols	Description
1.	V_{in}	Input Voltage to the Converter
2.	L_r	Resonating Inductance
3.	L_m	Magnetizing Inductance
4.	f_s	Switching Frequency
5.	f_r	Resonating Frequency
6.	C_r	Resonating Capacitance
7.	C_o	Output Capacitance
8.	i_{Lm}	Magnetizing current
9.	i_s	Secondary current of the converter
10.	i_r	Resonating Current
11.	V_o	Output Voltage of Converter
12.	V_{dc}	DC Link Voltage
13.	R_{ac}	AC Resistance referred to primary of converter
14.	R_o	Actual output Resistance
15.	n	Number of turns
16.	Q	Quality Factor
17.	M	Gain of the Converter
18.	V_g, I_g	Grid Voltage, Grid Current
19.	R, L	Parallel Load Resistance and Inductance
20.	L_c	Input Side Filter Inductance
21.	I_{bat}	Battery Current

CHAPTER 1
LITERATURE SURVEY

1.1 Introduction of EVs

It is anticipated that between 2009 and 2036, the worldwide energy consumption attributed to transport will rise by almost 45%. This leads that majority of energy is required to operate large number of appliances with proper requirement. The majority (63%) of the energy consumption is based on the substitute of oil, diesel and other fossil fuel consumption between 2015 and 2035. The Acid rain, ozone degradation, climate changing, rising air pollution, and global warming have all been brought on by the burning of non-renewable, fossil fuels that are a finite resource. Researchers, governments, industry, and the general public are therefore very interested in innovative technology for alternative vehicles these days that completely replace these vehicles [1].

Internal combustion (IC) engines have been the only type of engines used in international transportation networks for a very long period. Diesel, gasoline serve as the primary sources of energy for the vehicle engine in conventional transportation propulsion system. Due to the hazardous CO_2 emissions emitted during combustion, the usage of such fuels results in health issues. As a result, recent research and attention have focused heavily on electric and hybrid vehicles (HEV) [2]. It is done in order to reduce the hazardous gases emitted during the combustion of these fuels and pave the way to a clean and energy-efficient transportation system. The requirement of power is fulfilled in the EV transportation, rechargeable batteries are essential in hybrid and electric automobiles. additional, less expensive EVs which are driven by lead acid and lithium-ion batteries.

Internal combustion engines (ICEs) are not used to power EVs (EVs), which are instead fueled directly by an energy storage source. EVs are more environmentally friendly than normal fossil fuel-powered vehicles since they use less fuel and produce less air pollution and carbon emissions. As a result, EVs are becoming more and more liked globally [3] [4].

The fast-charging mechanism is the current demand of EV nowadays. To minimize the time of charging for an EV, fast charging stations are installed and used suitably. The choice of battery packs are important for designing efficient and effective design for EV. Modern lithium and lead acid batteries packs, which use fast charging that providing longer travel distances with shorter duration of charging time. Thus, effective and quick charging method is always a

topic of research area for EV batteries [5].

There are multiple advantages of EVs. These technologies can be employed as energy storage units in vehicle-to-grid (V2G) applications in addition to conventional grid-to-vehicle (G2V) charging systems [3]. This helps to alleviate environmental deprivation and the fossil fuel problem. The core idea behind V2G based technology is to use automobiles as energy storage systems and supply the grid with electricity to help it out when voltage and frequency dips occur. This support may be crucial when a significant amount of electricity gets generated by renewable energy sources such Tidal, wind, solar [8].

1.2 Batteries for EVs

There are some technological constraints which are always considered during its selection. It includes higher costs than petrol engines of comparable size, lengthy charging periods, constrained battery life, and restricted travel distance on a single charge which are considered for the research point of view. The most crucial factors for an EV battery are its lifetime, dependability, affordability, and power density (power, volume, and weight).

The actual current, which is measured in Ampere-hours that determines the rate of charging and discharging rate of a particular battery. There are two methods to evaluate the battery span life of battery: the shortest possible life span and the total number of charging/discharging cycles. An automobile battery is normally expected to be utilized 8–12 years. The overall trade-offs must be taken into consideration, an EV battery should be able to satisfy each of these requirements while remaining affordable, as the high cost of batteries has historically been a major barrier to the widespread adoption of EVs.

Currently, lead-acid batteries, nickel metal hydride (NiMH) batteries, and lithium-ion (Li-ion) batteries—three major battery technologies—are widely used in EVs. The lead-acid batteries are provided in the earliest electric cars, such as the GM EV1. It can react fast to load variations due to its high discharge power capacity. Meanwhile, the cost is fair because of the rapid advancement of technology. It is not suited for today's EVs because of its heavy weight and short lifespan as a result of deep discharging degradation.

Both the Honda Insight and the Toyota Prius employ NiMH batteries [6]. The charge/discharge processes are less complicated in a NiMH battery than in a lead-acid battery, it delivers a higher power density. Due to the high-density component, the NiMH battery in the EV offers a driving range that is twice as long as the equivalent lead-acid battery [8].

Since a NiMH type of batteries are able to tolerate both fast overcharges and severe rate of discharging, that provides a far better life cycle to it. The NiMH battery's high charge

acceptance capacity and low internal resistance result in a higher charging efficiency [5,6]. The major drawback of NiMH type of batteries is that it has a quick self-discharge rate, that causes the battery to lose charge even while it is not in use. Additionally, it is more expensive and less capable of accepting charges in hot environments.[7]

Li-ion batteries have emerged as primary storage of energy in recent versions of EVs, like the Nissan Leaf. Despite the fact that the Li-ion battery has solved many of the issues of battery like cell balance issues, cell life, cooling performance, safety, and cost [8]. When compared to other rechargeable batteries, it offers multiple advantages.

As compared to lead acid batteries (6 to 10 percent per year) and nickel metal hydride (NiMH) batteries (40 percent per year). Because of this, the Lithium-ion battery provides longer lifespan than other battery technologies [9]. The discharge curve of a lithium-ion battery is also uniformly flat. It is well known that, particularly for high-power applications, a serious issue may develop near the conclusion of the discharge cycle if the battery's power output reduces rapidly. For around 80% of the discharge cycle, the lithium-ion battery, as shown in Fig. 1.1, provides basically constant current and constant voltage (corresponding stable power) [10].

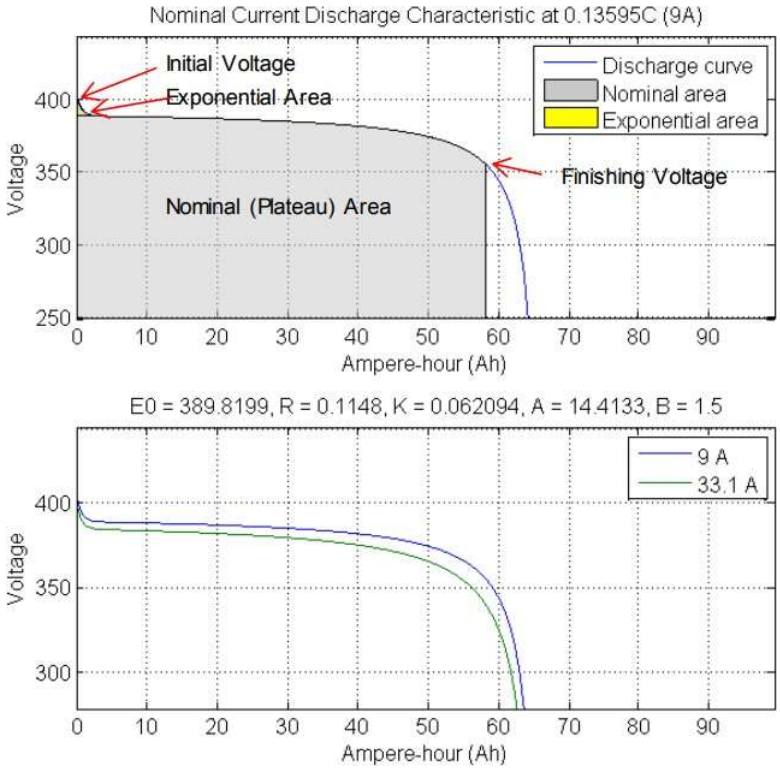

Fig.1.1 The Li-ion battery discharge characteristic [2][4]

1.3 Battery charging Technology

The performance and utility of Battery is influenced by charging and discharging characteristics and the technology implemented for designing it. As a result, the working criteria of battery charging and discharging are crucial for the entire EV system [11].

1.3.1 Charging strategy

There are various techniques of charging, including constant current (CC), constant voltage (CV), constant power, taper current, and others. Most fundamental method of charging a battery is with a constant voltage charger. It operates with appropriate value current to maintain a steady rating of voltage required by the battery [11]. It requires additional technology that safeguard it. The maximum current for fast charging is often fed into the battery by a constant current charger, which causes the battery voltage to rise linearly over time. Large and expensive batteries are often charged slowly using a continuous power charger. The most important limitation for charging is that it always requires special attention.[12]

For Li-ion batteries, the constant current-constant voltage (CC-CV) charging method is frequently employed. There are two steps to the charging process in this CC-CV charging profile: CC mode and CV mode. The first step is the CC mode, in which the battery voltage grows quickly to its rated maximum level while the current is regulated at a constant value (usually the utmost current that the battery can tolerate without harm). Constant current charging carried out indefinitely will cause overcharging and excessive heating, perhaps harming the battery.

This is prevented as the level of voltage reaches a particular level of voltage that is going to start the charging process of battery. The process of charging is inclined towards constant voltage mode configuration, during which the battery voltage is maintained at a constant value while the battery is gently charged. As value of charging current touches, a particular value of current that is less that the predefined value of current, the process that is utilized in charging is terminated to prevent overcharging [12][13].

The typical cells of Li-ion battery having a maximum charging voltage is 3.2V or 4.6V. As the level of battery voltage exceeds 95% of state of charge (SOC), the current begins to decline and CV stage starts.

1.3.2 Charging level of power

According to different power ratings and charging times, battery chargers are divided mainly into three types

1. Level 1 for slow (domestic) charging
2. Level 2 for primary charging
3. Level 3 for fast charging (usually using DC voltage).

The lowest level of EV charging is Level 1. It has a range of 4 to 5 miles after an hour of charging and is powered by a regular 120 V household outlet. A Level 1 EVSE wire set is typically included by EV manufacturers; therefore, no additional hardware is required for charging. A fully discharged EV battery needs roughly 20 hours to recharge. North, South, and Central America, Europe, and a significant portion of the world are the only places that employ a 220 V inventory structure. This kind of installation requires a charging mechanism that costs between 520 and 900 dollars [14].

A 208 V charging station outside or a private 220 V supply system are used by level 2 charging equipment. A 3.3 KW on-board charger can provide around 15 miles of range in an hour of charging. On the other side, a 6.6 KW on-board charger may cover 30 miles in the time it takes to charge. In order to speed up recharging, Level 2 EVSEs use equipment that is specifically made for that purpose and necessitate expert electrical installation using a dedicated electrical line. The price range for the Level 2 charging system will be between 77k to 232k Indian rupees [1000-3000 USD].

For Level 3 charging, a 440 V AC supply system is necessary. After charging, this kind of charger may cover 60–80 miles in time span of 25–35 minutes. In order to directly power the EV battery pack, the DCFC converts AC electricity to DC. Only commercial use qualifies for this level of invoicing, not household use. The price of execution is between 30000 and 160000 USD or 23 lakh and 1,24 crores [15].

1.3.3 Off- Board and On-Board Charger

On-board and off-board categories are frequently used to categories battery chargers for electric cars. Off-board chargers, often referred to as standalone fast-charging stations, provide high-power charging at a quick pace, operating similarly to filling stations for liquid fuel cars. Off-board charging stations are often installed in public spaces like parking lots, shopping centers, and highway facilities. These stations can significantly increase the range of pure-battery EVs. The constraints on size, weight, and space needed to construct such an off-board station are eased; yet, these stations demand significant funding and prolonged construction time [16].

On the other hand, on-board chargers, which are integrated into the vehicles, offer moderate charging times of 6–16 hours at low power levels of 2–20 kW. On-board chargers make it easy to charge EVs when they are connected to a home utility connection overnight. The cost of the charger won't be as high as an off-board recharge station because it can be incorporated within the EV. On-board charging is still a viable option because of its tiny form, simplicity of use, and low cost despite the fact that size, weight, and space restrictions restrict the input power level and make charging slow [17].

On-board chargers frequently use Level 1 and Level 2, which are designed to be fitted in the vehicle, in accordance with the SAE J1772 standard, while off-board chargers typically use Level 3.

The comparison is based upon the power, level type and charging time of EV chargers which are utilized to operate in different conditions [18].

1.4. Power converters for EV battery charging

The converter is designed as per the application, the flowchart representing the converter

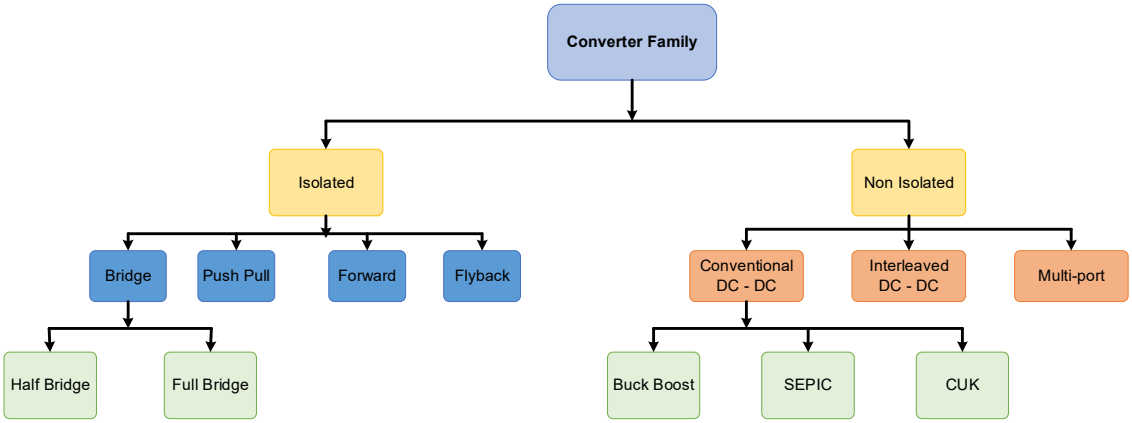

Fig.1.2 Converter Family Tree

1.4.1 Non-Isolated converters

For applications involving the generation of renewable energy, DC-DC converters are widely used. However, non-isolated DC-DC converter topologies are superior to isolated converter topologies in terms of benefits. These topologies are nevertheless more practical to combine with renewable energy applications than their isolated converter counterparts, while having a few minor drawbacks such a high duty cycle ratio, poor voltage gain, and extra circuitry. Non-isolated converters often have less application flexibility than their isolated counterparts. They do, however, provide a number of advantages for designers in situations when isolation is not necessary [15].

A non-isolated converter normally is smaller and lighter since it does not need a transformer or any other kind of physical separation between the input and output. Since there are no transformer losses to account for, it also increases efficiency. Since no isolation is necessary for any signals that cross the isolation border, eliminating the requirement for opt isolators and/or signal transformers, the design of non-isolated converters is often simpler. Non-isolated converters often cost less due to the decrease in BOM [18].

1.4.2 Isolated converters

Galvanic isolation, which denotes the absence of a metallic or direct conduction path between two components of the circuit, is what isolation in the context of DC/DC converters signifies. The isolation may be necessary for circuit functionality, safety, or both. It will always act as a barrier between the input stage and the output stage.

In a non-isolated converter, the input and output stages share a single ground, whereas in an isolated converter, the input and output stages have separate grounds. Utilizing a transformer in the circuit to transfer power via electromagnetic radiation typically results in isolation. Although there is some efficiency loss with this, it can be mitigated with a correctly built transformer. Signals must occasionally be routed across the isolation boundary. This is especially important for regulated devices since they need a feedback signal. These signals must also be segregated in order to maintain the separation. Small signal transformers can be used for AC transmissions, while optocouplers are typically utilized for DC signals to provide isolation [19]. Electrical insulation between the conductors, usually in the form of tape or another non-conductive substance, is used to provide isolation. It is typically stated as a voltage, and increasing the voltage can cause the isolation to fail [20].

CHAPTER 2

LLC RESONANT CONVERTER

2.1 Introduction

There are several kinds of topologies that provide the best operation of resonant-converter, and they are fundamentally identical for the operation point of view. There are power switches which produce a square waveform of electrical quantities that is passed through the resonant circuit to achieve resonance. The resonant circuit generates energy between inductor and capacitor which is utilized to achieve the resonance condition of the circuit [21].

There are some fundamental forms of LLC converter in which series and parallel resonant converter designs are widely utilized. These converters are best suited for getting the isolation between the circuit. The resonance is achieved by the impedance offered by the tank circuit present between inverter and rectifier end of the converter. The variation of frequency provides them a wide range of operation that makes it out with respect to all the converters. The entire input voltage of converter is shared between the impedance offered by the tank circuit and load. The converter design is illustrated by the fig 2.1 and fig 2.2.

2.1.1. Series Resonant Converter

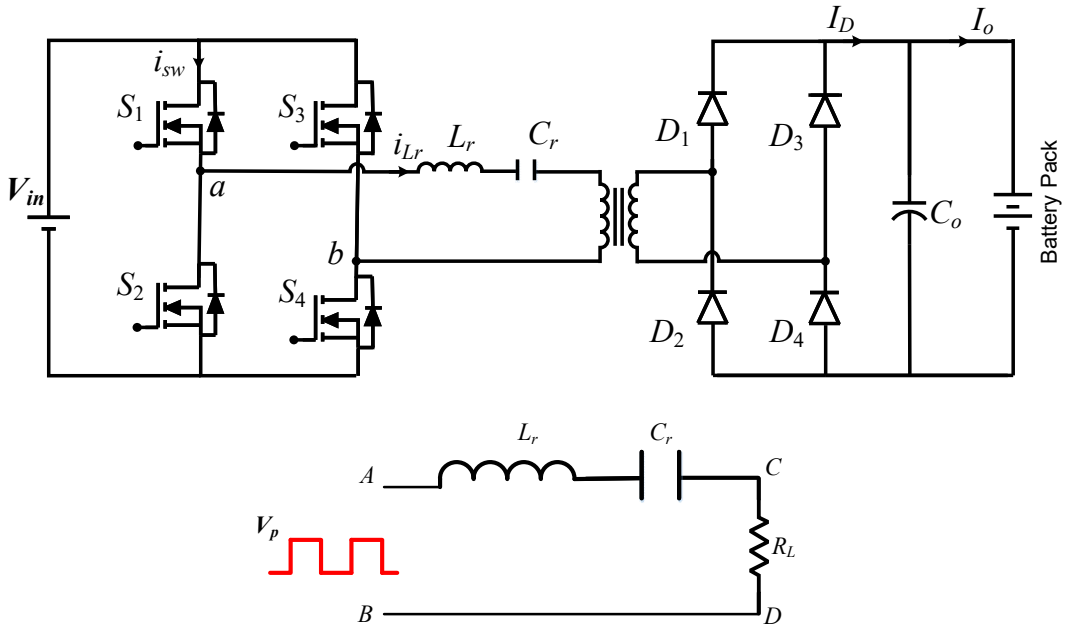

Fig 2.1 Series resonant converter

2.1.2. Parallel resonant converter

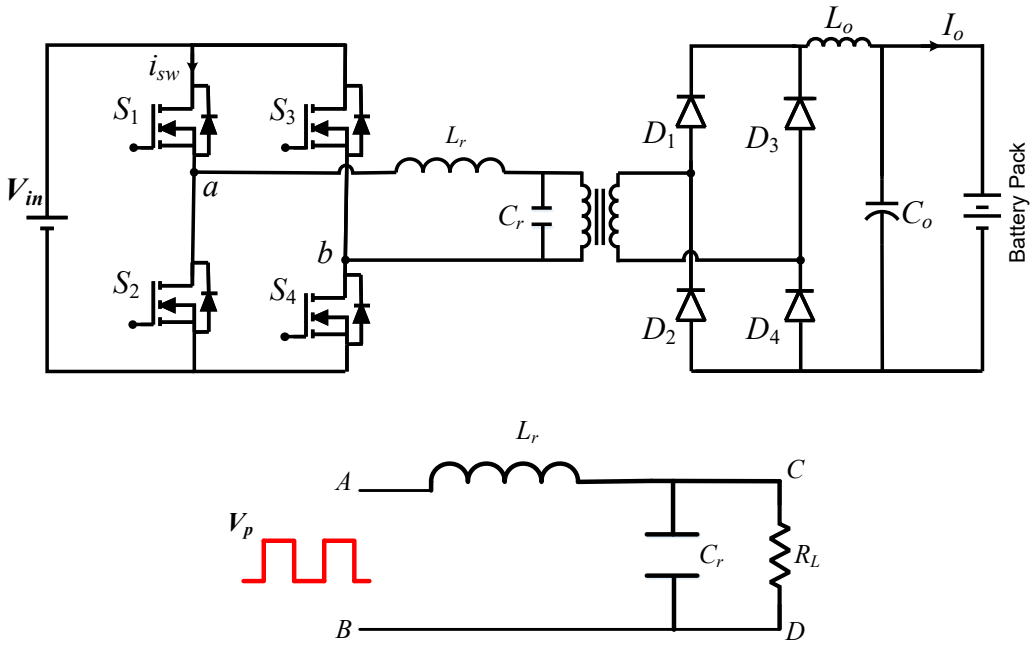

Fig 2.2 Parallel resonant converter

2.1.3. LLC Resonant converter

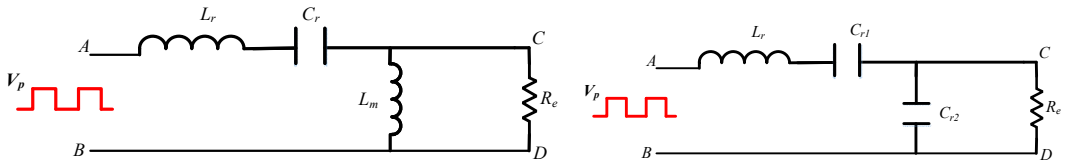

Fig 2.3 Topology defines LLC resonant converter design

A converter known as a series-parallel resonant converter (SPRC), which combines both of the designs. It is designed to overcome these constraints. One variation of this arrangement, as depicted in Fig. 2.3, employs an LCC layout, which is one inductor and two capacitors. By incorporating more resonant frequencies, these basic limitations can be minimized. There is necessitates the use of two separate physical capacitors, which are enormous and expensive due to the high AC currents [22].

The SPRC can be modified to employ two inductors and one capacitor, making an LLC resonant converter, in order to obtain comparable properties without affecting the physical component count. Compared to traditional designs of converter, these designs of converter provide numerous advantages. For instance, it can adjust the output while retaining outstanding efficiency.

Zero voltage switching (ZVS) is also possible over the full operational range. The method of designing that king of topology will next be discussed in this chapter [23][24].

2.1.4. Bridge configuration resonant converter

There is always a huge demand of efficient power and high-power density as power conversion technology advances. For many powers supply and energy-related applications, DC-DC power conversion is a necessary stage. The power capabilities of the DC-DC converters are particularly challenged in all the sectors. Resonant power converter generally contains three stages that includes square wave generator, resonant tank circuit and diode bridge rectifier with filter capacitance [25].

The pulse width modulated gating signal is applied using PI controller (approx. 50% duty cycle) to switches S_1, S_4, and S_2, S_3. Square wave generator creates a voltage that is square in nature. Typically, a little dead period is included in between each subsequent transition.

The square waveform is achieved by using a bridge converter design. The magnetizing inductance component of the transformer, leakage inductance and capacitor make up the resonant network. The magnetizing branch of the inductance, which serves as a shunt inductor is represented by L_m, L_r representing value of resonant inductor, C_r representing value of resonant capacitor respectively.

This resonant network helps to achieve resonance condition. Resonant network filters out higher harmonic currents and helps to achieve resonance and receives a square nature of voltage waveform through inverter end. The resonance condition is quite crucial in designing the converter that maintains the switching losses. This resonance condition is achieved by the suitable values of resonant inductor and resonant capacitor with shunt inductance of transformer connected in parallel.

At rectifier end of the resonant converter creates dc voltage from the ac input. The filter capacitance at the output of the rectifier is used to remove high frequency ripples. At the rectifier end is connected with battery pack for the application of charging [26].

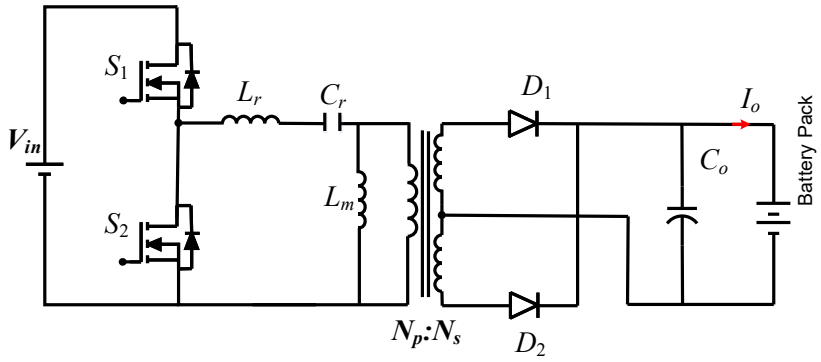

Fig 2.4 Half bridge LLC resonant converter

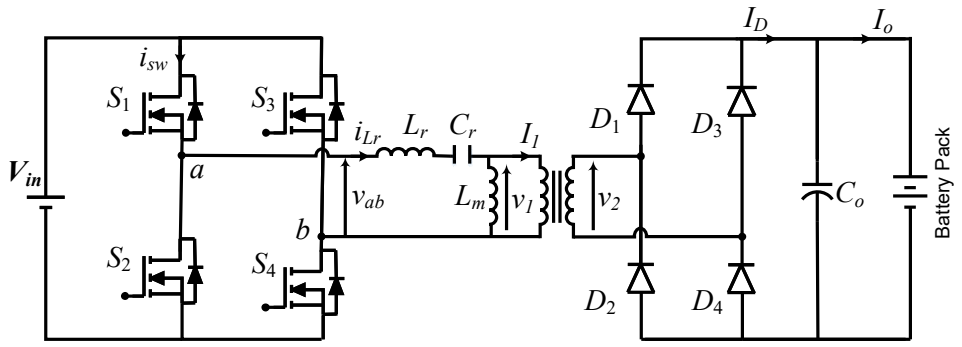

Fig 2.5 Full bridge LLC resonant converter

2.2 Modes of operation of Full Bridge LLC Resonant Converter

Modes of operation of proposed converter

Case 1. Forward mode:

As shown in Fig 2.6(a), S_1, S_4 switch on at t = t_1 that allows the input current to pass to load though resonant tank circuit and achieves ZVS at the end. The ZVS state allows to mitigate the switching losses and improves the efficiency

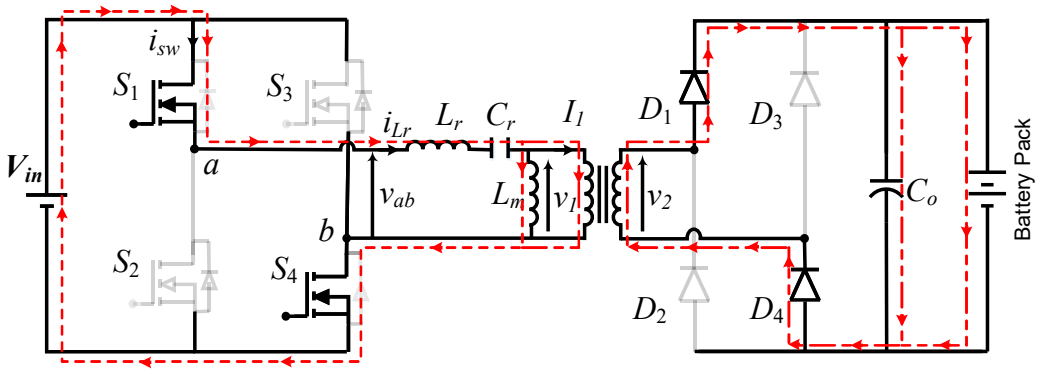

(a)

Case 2: Reverse mode

As shown in Fig 2.6(b), S_2, S_3 switches are operated at t = t_2 and achieve ZVS while S_1, S_4 remain at off state. The primary current reaches to load in the same manner that allows the battery to charge at the desired level of voltage.

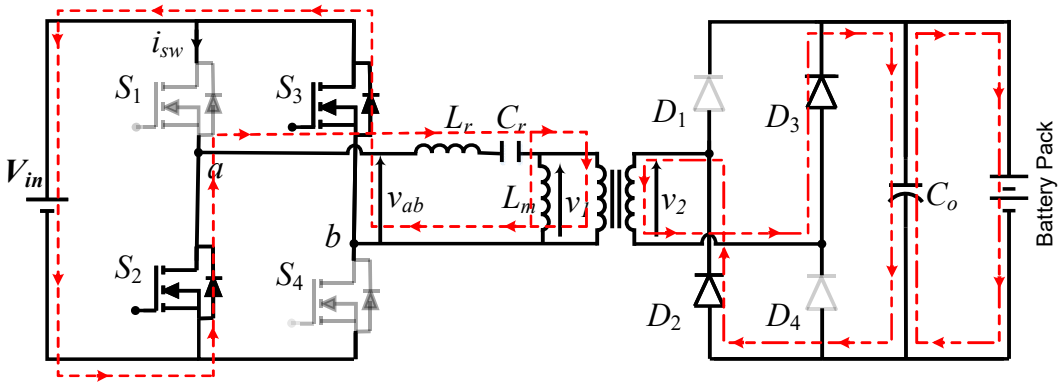

(b)

Case 3: Dead Band region

As shown in Fig 2.6(c), S_1, S_4 are cut off at t_3 while S_2, S_3 still remain at the cut off state. This forms a dead time region where all the switches are in their off state.

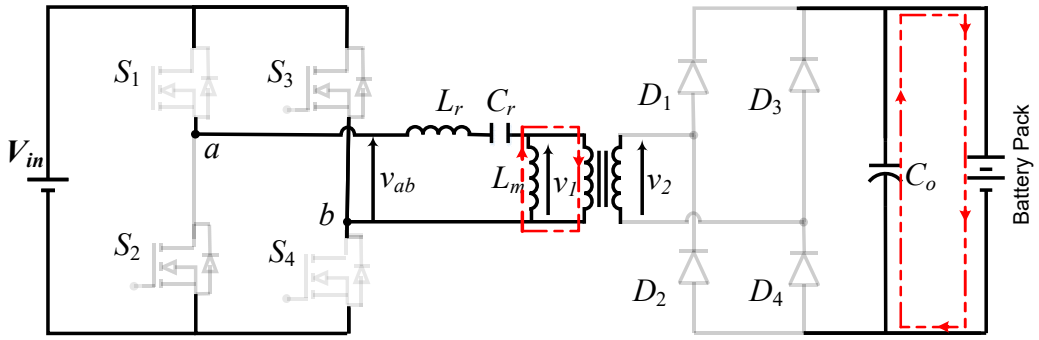

(c)

As shown in Fig 2.6(d), The switching waveform is defining the different mode of operation depending upon the signal applied to gate signal of switches.

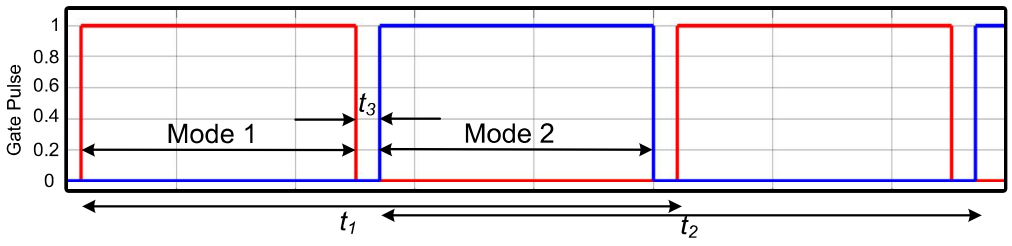

(d)

Fig 2.6. (a)Switching condition of S_1, S_4(Mode1) (b) Switching condition of S_2, S_3(Mode2) (c) Dead band region (d) Switching waveform

2.3 Design Calculations

Equations and Parameter Value Calculations

$$\frac{V_{o1}}{V_{in1}} = \frac{(8/\pi^2)\omega_x^2}{\sqrt{(\omega_x^2 + (\frac{L_r}{L_m}(\omega_x^2 - 1))^2 + Q^2\omega_x^2(\omega_x^2 - 1)^2}} \quad (1)$$

It defines the relation among the Gain(K) of converter and the normalized frequency (Fn). Gain equation gives the value of Quality factor and Ratio of magnetizing branch of inductance to resonant branch of inductance.

$Q = \frac{\sqrt{L_r/C_r}}{R}$ Q is Quality Factor.

$R_{ac} = \frac{8N_r^2}{\pi^2 N_s^2}.R_o$ Rac is Equivalent Resistance.

$F_n = \frac{f_s}{f_r}$ F_n is Normalized Switching Frequency.

$f_r = \frac{1}{2\pi\sqrt{L_r.C_r}}$ fr is Resonant Frequency.

$m = \frac{L_r + L_m}{L_r}$ m is ratio of Magnetizing Inductance to Resonant Inductance.

For designing resonant converter, minimum and maximum value of voltage gain of the converter is selected with proper turns ratio of transformer. The nominal value of voltage gain is considered to be unity.

$$M_{nom} = 1; \quad \frac{N_p}{N_s} = 1.25 \quad (1)$$

where;

M_{nom} = nominal voltage gain,

N_p = 120 and N_s = 96 are the primary and secondary turn ratio.

$$M_{\max} = \left(\frac{V_{in\_nom}}{V_{in\_\min}}\right) M_{nom} = 1.04 \quad (2a)$$

$$M_{\min} = \left(\frac{V_{in\_nom}}{V_{in\_\max}}\right) M_{nom} = 0.96 \quad (2b)$$

where;

M_{max} = maximum voltage gain,

V_{in_nom}, V_{in_min}, V_{in_max} are nominal, minimum and maximum input voltages respectively.

The proper values of gain are obtained by selecting the nominal voltage, min nominal voltage and max nominal voltage of the converter specifications. The values of resonant tank circuit are calculated by selecting quality factor (Q_{max}) and gain (m) value. The value of Q_{max} is considered as 0.4 as shown in Fig. 4. The value if m is considered high due to following reasons.

- Higher the value of efficiency
- Higher magnetizing inductance
- Lower magnetizing circulating current

The proper values of Q_{max} and m specifies the performance of converter as well as soft switching behavior. The switching of the converter decides power losses that affects efficiency of converter. Higher the switching losses, decreases the efficiency and performance at higher frequency operation. Converters at such high frequency of 100 kHz require fast and instant switching which enables the resonant mode of operation. This high frequency operation also provides low value of current/voltage stress at switches and achieves ZVS & ZCS operation to mitigate switching losses

Step1: Selecting the Q_{max} value; i.e., $Q_{max} = 0.4$

Step 2: Selecting the m value; 0i.e., $m = 6.3$.

Step3: Calculating resonant components value

$$R_e = \left(\frac{8}{\pi^2}\right) \times \left(\frac{N_p}{N_s}\right)^2 \times \left(\frac{V_o^2}{P_o}\right) = 22.52 \text{ ohms} \tag{3}$$

Step 4: Calculation of resonant capacitance:

$$C_r = \frac{1}{2\pi Q f_o R_{ac}} = 19.03nF \tag{4}$$

Step 5: Calculation of resonant inductance:

$$L_r = \frac{1}{4\pi^2 f_o^2 C_r} = 120\mu H \tag{5}$$

The value of L_r, C_r defines the performance and resonance condition of tank circuit which is crucial part of designing for resonant converter and achieving resonance condition.

The specification of resonant converter is depicted in Table I.

Table I. Specifications of resonant Converter

Parameters	Variables	Values
DC-input Voltage	V_d	120 V
Resonant Frequency	f_r	89.7 kHz
Switching Frequency	f_{sw}	100 kHz
Resonant Inductance	L_r	120 µH
Resonant Capacitance	C_r	22.52 nF
Filter Capacitance	C_o	470 µF
Output current	I_o	15.625 A
Battery capacity		15.625 Ah
Battery type		Lithium ion (C1 Type)
Battery nominal voltage	V_b	96
Initial state of charge		45%

The normalized operating switching frequency is greater than the operating resonant switching frequency which forces the designing parameter of converter to operate in buck mode of operation. Thus, battery rating of 96 volts is charged by the dc input voltage of 120 volts. The filter capacitance is considered at high value of 470µF; which eliminates the higher order harmonics at output voltage [27]. The elimination of harmonics improves the waveform of converter and provides a better form of regulation throughout. Thus, it is very crucial to eliminate all such harmonics that deteriorate the waveform. The resonance condition is also achieved to mitigate the losses of the converter at such high frequency of 100 kHz. The high frequency of operation is adopted due to great demand and better optimization of power electronic converters.

The gain of converter plays vital role in the designing part. Gain of the converter is compared with respect to range of frequencies for operation. This describes the operating frequency of the converter at the best value of quality factor. Gain of the converter is the function of frequency and value of *m* respectively [28]. This also describes the region at which resonant converter is operating suitably with minimum losses.

2.4 Zero voltage Switching

Converters can implement soft switching in a number of different ways.The goal is to produce a forced swing using LC transients. As a result, soft switching activates and deactivates the electrical switch using an LC resonant circuit. The current and voltage waveform intersection is minimized by controlling the switching timing[. It is crucial to eliminate power losses to improve efficiency. Moreover, it helps in lowering inductance, switching losses, and diode losses [29][30]. ZVS and ZCS are switched as part of the process. In fact, the electronic switch utilizes the resonance phenomenon to switch on and off under soft switching conditions. The fact that switches switches on and switches off respectively at zero (or close to zero) voltage or current decreases switching losses and improves efficiency of converter.

The current flowing through the switches of resonant converter lags the input voltage during the inductive region operation. As a result, direction of resonant current cannot abruptly change when the switching state changes and instead continues to flow in the original direction. The converter uses zero voltage switching as a soft switch. Soft switching is highly helpful in high efficiency applications because ZVS lowers the switching losses in the circuit at the moment of switching.

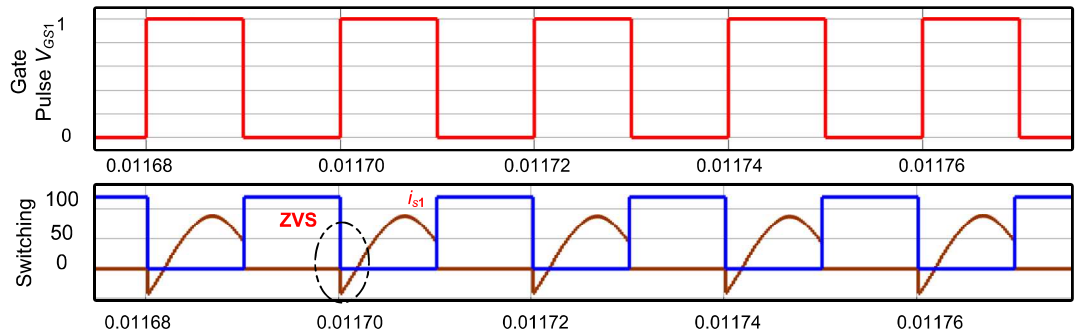

Fig 2.7 (a). Zero voltage switching along S1, S4 switches

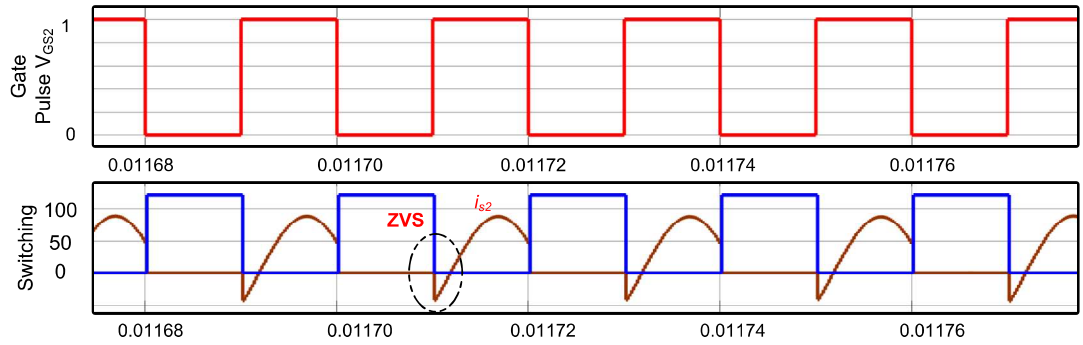

Fig 2.7 (b). Zero voltage switching along S2, S3 switches

CHAPTER 3

MATHEMATICAL MODELLING OF LLC RESONANTCONVERTER

3.1 Transfer function of Converter

The transfer function is defined as the ratio of Laplace Transform of output voltage to Laplace transform of input voltage with all initial conditions to be zero. The equivalent circuit is important to study further calculating the transfer function of converter, shown in fig 3.1

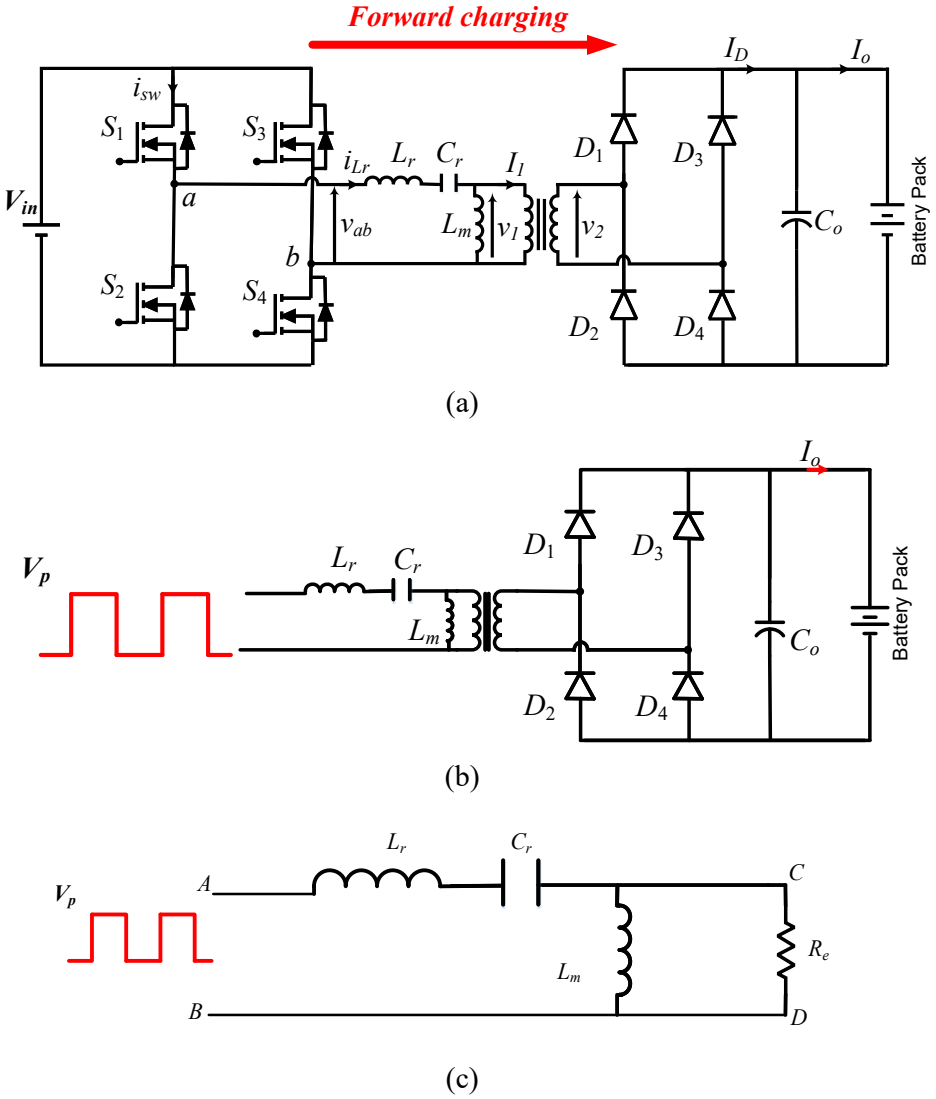

Fig 3.1 LLC resonant converter (a) connected with rechargable battery; (b) output of square wave connected with resonant tank fed rectifier circuit; (c) ac equivalent

circuit with R_{ac} load

3.2 Mathematical expression representing gain and frequency of converter

The transfer function of Full Bridge LLC resonant converter is represented by the ac equivalent circuit with R_{ac} load as mentioned in Fig. 3(c). It is represented by the voltage across CD terminals and voltage across AB terminals of the given circuit diagram and represented by Eq (3.1).

Where

$$X_{Lr} = \omega_{Lr}, X_{Cr} = 1/\omega_{Cr}, X_m = \omega L_m$$

$$\frac{V_{CD}}{V_{AB}} = \frac{jX_m R_e}{jX_m R_e + (jX_{Lr} - jX_{Cr})(jX_m R_e)} \tag{3.1}$$

$$\frac{V_{CD}}{V_{AB}} = \frac{1}{1 + j\frac{X_{Lr}}{R_e} - j\frac{X_{Cr}}{R_e} + \frac{X_{Lr}}{X_m} - \frac{X_{Cr}}{X_m}}$$

$$\frac{V_{CD}}{V_{AB}} = \frac{1}{(1 + \frac{X_{Lr}}{X_m} - \frac{X_{Cr}}{X_m}) + j(\frac{X_{Lr}}{R_e} - \frac{X_{Cr}}{R_e})}$$

$$\frac{V_{o1}}{V_{in1}} = \frac{8/\pi^2}{\sqrt{1 + (\frac{\omega L_r}{\omega_{Lm}} - \frac{1/\omega C_r}{\omega_{Lm}}) + (\frac{\omega L_r}{R_e} - \frac{1/\omega C_r}{R_e})^2}}$$

$$\frac{V_{o1}}{V_{in1}} = \frac{8/\pi^2}{\sqrt{(1 + \frac{L_r}{L_m} - \frac{L_r}{\omega^2 C_r L_r L_m})^2 + (\frac{\omega_{Lr}}{R_e} - \frac{1}{\omega C_r R_e})^2}} \tag{3.2}$$

Putting the value,

$$Q = \frac{\omega_o L_r}{R_e} = \frac{1}{\omega_o C_r R_e}$$

$$\omega_o = \frac{1}{\sqrt{L_r C_r}}, \omega_x = \frac{\omega}{\omega_o}$$

where ω_x is normalized switching frequency that is defined by ratio of switching to resonant frequency-

$$\frac{V_{o1}}{V_{in1}} = \frac{8/\pi^2}{\sqrt{(1+\frac{L_r}{L_m}(1-\frac{1}{\omega_x{}^2}))^2 + Q^2(\omega_x - \frac{1}{\omega_x})^2}}$$

$$\frac{V_{o1}}{V_{in1}} = \frac{(8/\pi^2)\omega_x{}^2}{\sqrt{(\omega_x{}^2 + (\frac{L_r}{L_m}(\omega_x{}^2 - 1))^2 + Q^2\omega_x{}^2(\omega_x{}^2 - 1)^2}}$$

$$\frac{V_{o1}}{V_{in1}} = \frac{(8/\pi^2)\omega_x{}^2}{\sqrt{(\omega_x{}^2 + (\frac{L_r}{L_m}(\omega_x{}^2 - 1))^2 + Q^2\omega_x{}^2(\omega_x{}^2 - 1)^2}} \quad (3.3)$$

Eq (3.3) shows the complete transfer function in terms of Quality factor, ratio of resonant and magnetizing inductance and operating frequency of the proposed converter. Based upon its number of curves are drawn at different values of m to decide the range of the Gain. This also defines the operating region during operation [31].

3.3 Gain of LLC resonant converter (Gain versus frequency variation of converter)

The gain of converter is the function of frequency which provides number of ways to analyze the LLC resonant converter. Eq (8) shows the complete transfer function in terms of Quality factor, ratio of resonant and magnetizing inductance and operating frequency of the proposed converter. Based upon its number of curves are drawn at different values of m to decide the range of the Gain [32][35]. This also defines the operating region during operation.

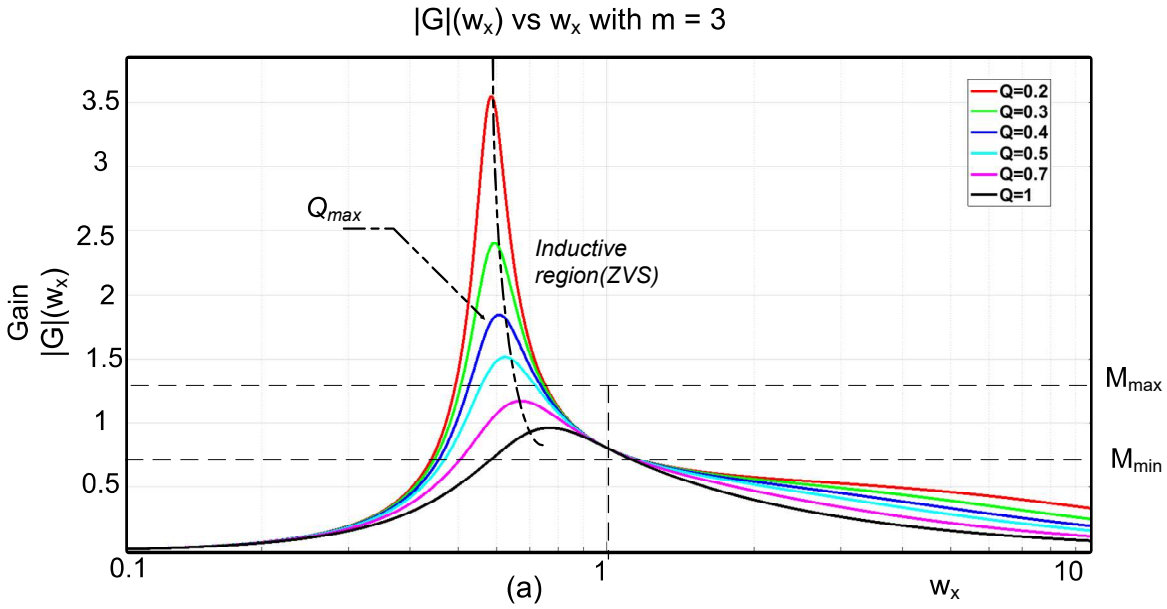

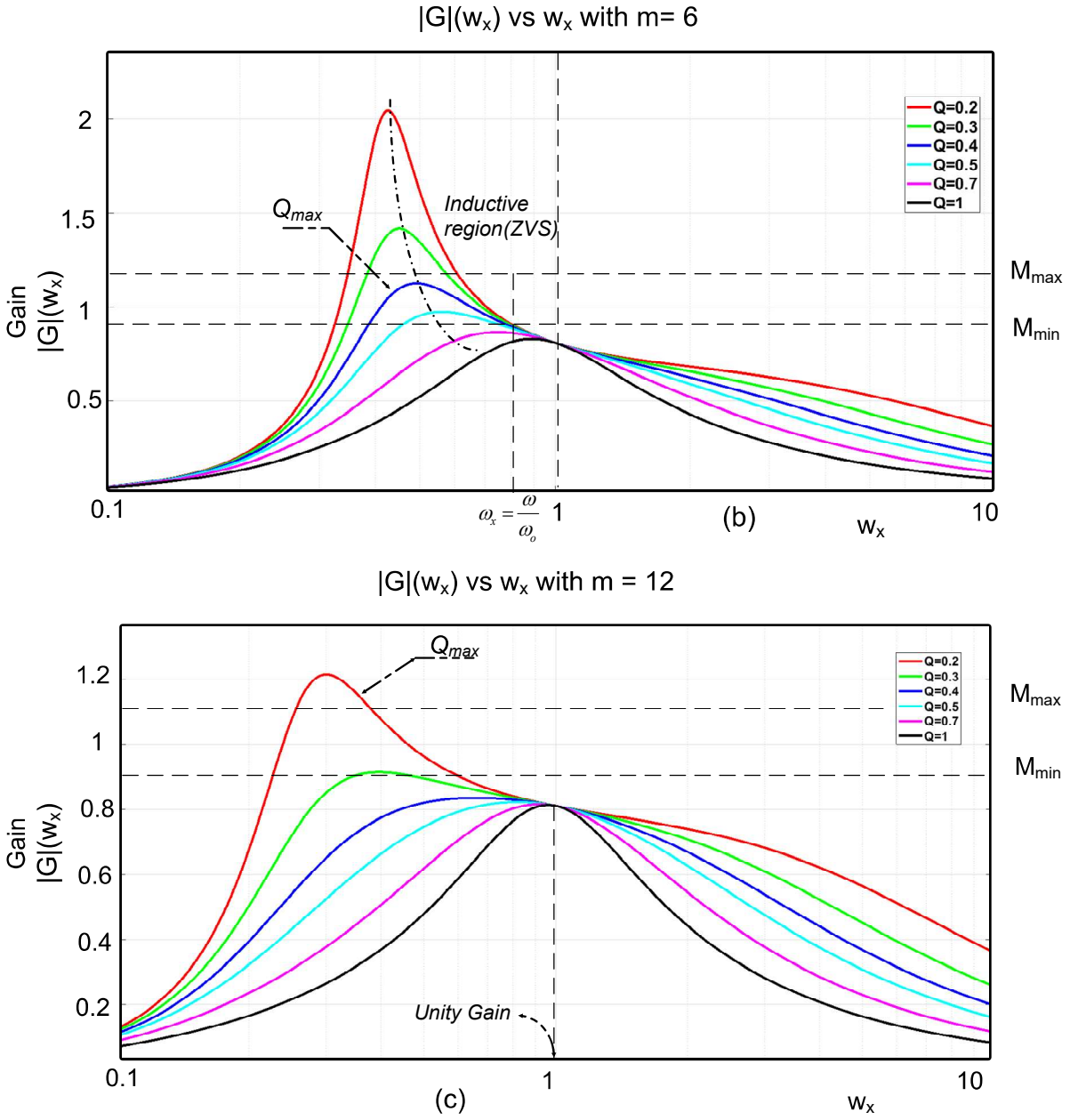

Fig 3.2. Gain versus frequency curve of resonant converter at *(a) m = 3, Q = 0.7 (b) m = 6, Q = 0.4 (c) m = 12, Q = 0.2.*

The curve in Fig. 3.2 is plotted at different values of m that depicts the operating region of the converter at a specific value of *Q*. The converter is operating in inductive region that is utilized to achieve ZVS condition. The maximum value of *Q* is represented by Q_{max}. As the *Q* and frequency changes, the operating region of converter also changes. Thus, it is very crucial to optimize the quality factor value of Q_{max} for better operating condition and achieving resonance [33]. The steps to design the LLC converter is presented in Fig. 5.

The load independent gain characteristics offered by LLC-resonant converter in lagging region helps to sustain ZVS and constant switching frequency operation.The parallel inductor

placed parallel to transformer is crucial for maintaining ZVS under light load conditions and maintaining the magnitude of inrush current at the beginning.

This section describes how design factors influence voltage regulation and efficiency performance of resonant converter. It simplifies the design and helps to choose the values of converter that performs resonance. The final design objective is to meet gain requirement for all line and load regulations during charging the battery. These steps are executed to designing the converter which is suitable to operate at wide range of frequencies as well as different loading conditions that made it suitable for EV charging applications. Soft switching and resonance condition is obtained by resonant tank circuit. The PI controller is going to be tuned perfectly for maintain constant current at the output side of converter during charging [34][35].

3.4 Resonance Behavior of converter (Buck and Boost mode of operation)

LLC operation can be categorized into three modes based on switchingfrequency as indicated below

- $\mathbf{f_s = f_r}$ (Resonance Mode)
- $\mathbf{f_s > f_r}$ **(**Buck Mode)
- $\mathbf{f_s < f_r}$ (Boost Mode)

Case 1. At Resonant frequency, $f_s = f_r$: The half cycle of switching delivers power, so each half of the switching cycle is involved for the full operation of the power supply. At half cycle of switching, the rectifier current is zero, and the magnetizing current is achieved by the resonant inductor current. Since the resonant tank has unity gain and is the designed for most optimal operation. The efficiency at this point and the transformer turns ratio is designed so that the converter may also operate at this point for nominal input and output voltages [37].

Case 2. Above resonant frequency, $f_s > f_r$: Each half's switching cycle involves a small amount of power delivery action, which is analogous to resonant frequency operation. Additionally, before the resonant half cycle is finished, the second half of the switching cycle starts. Secondary rectifier diodes are harmed by strong commutation, whereas primary side MOSFETs experiences a great turn-off loss. This case of operation is intended for buck operation or step-down gain is required due to a higher input voltage rating.

Case 3. Below resonant frequency, $f_s < f_r$: Power delivery occurs during each half of the switching cycle. When the switching half cycle is completed, the freewheeling action starts and lasts until the magnetising current is reached by the resonant inductor current I_{Lr}. The circulating current increases conduction losses on the main side of converter. Converter runs in this mode when a step-up or boost operation is required due to a lower input voltage [37].

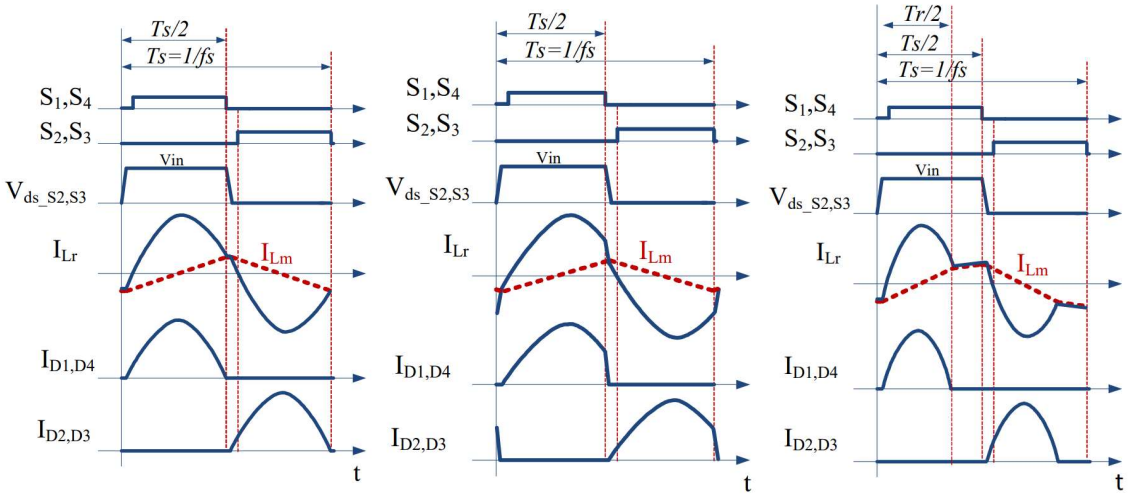

Fig. 3.3. a) Resonance mode, b) Buck mode, c) Boost mode operation of LLC resonant converter [38]

CHAPTER 4

BATTERY CHARGING TOPOLOGY

4.1 Converter topologies for EV Charging

The primary objective of this project is to build and analyze a high-efficiency charging system for EVs that can operate over a broad range of battery voltages. The basic design would be the LLC resonant converter. The main objective is to significantly enhance the power quality at the converter's supply side by working on the following areas:

1). Behavior of LLC resonant converter

The LLC resonant converter should be examined for various operating modes in order to determine the best mode of operation in order to construct an ideal battery charger.

2) Analysis of dc-dc converter for EV charging

The problem of continuous charging may overheat the batteries which is resolved by proper tuning of PI controller

There are multiple converter topologies which provide the EV charging at different levels

4.2 Full Bridge resonant converter

LLC resonant converter offers numerous advantages, including the capacity to maintain the output parameters constant over a large range of extension of load and line fluctuations with only a modest variation in switching frequency. Over the full operational range, it can accomplish zero voltage switching (ZVS). To achieve soft switching, all necessary parasitic elements of semiconductor devices are used [39][40]. It is easier to charge the batteries through full-bridge inductor-inductor-capacitor (LLC) resonant dc-dc converter.

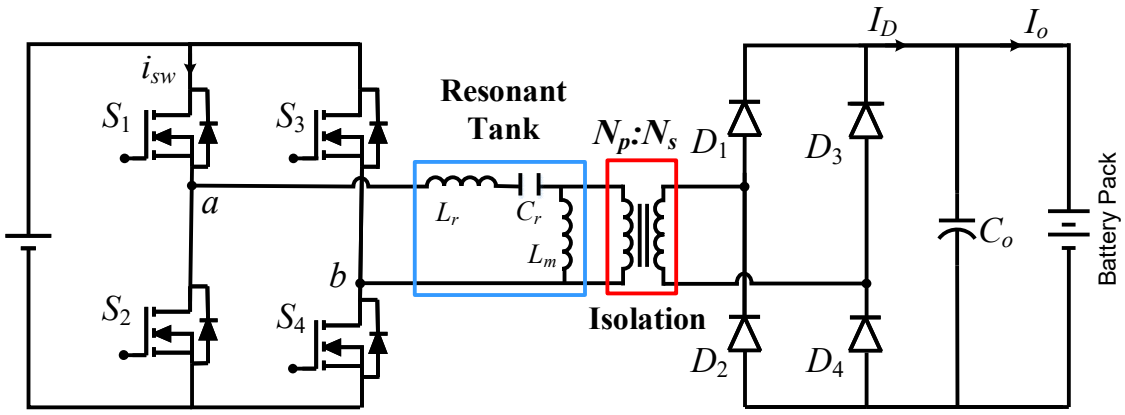

Fig. 4.1 Full Bridge LLC resonant converter

4.3 Dual active bridge converter

Dual active bridge converter performs operations in both the directions as diodes are replaced by switches. This allows the converter to performs charging and discharging applications throughout.

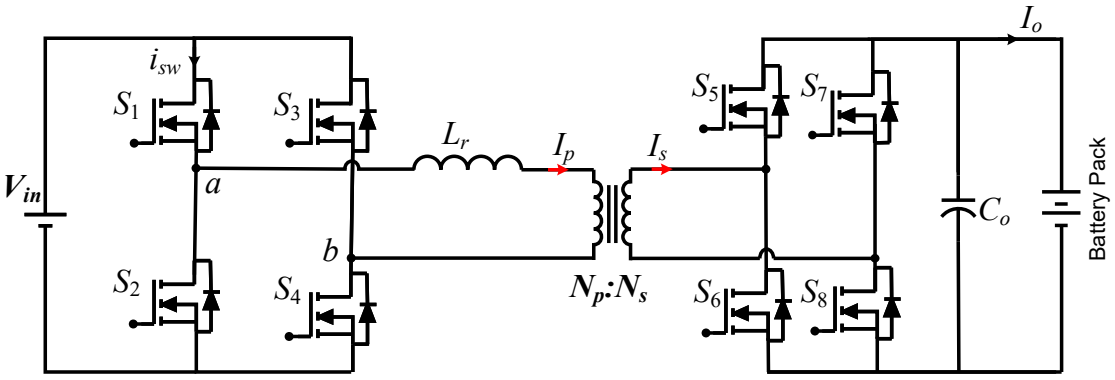

Fig. 4.2 Dual active bridge converter

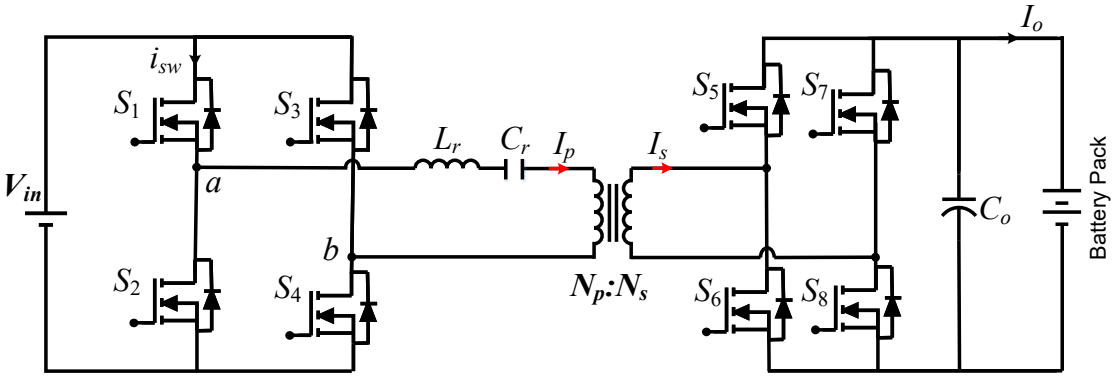

Fig. 4.3 Dual active bridge series resonant converter

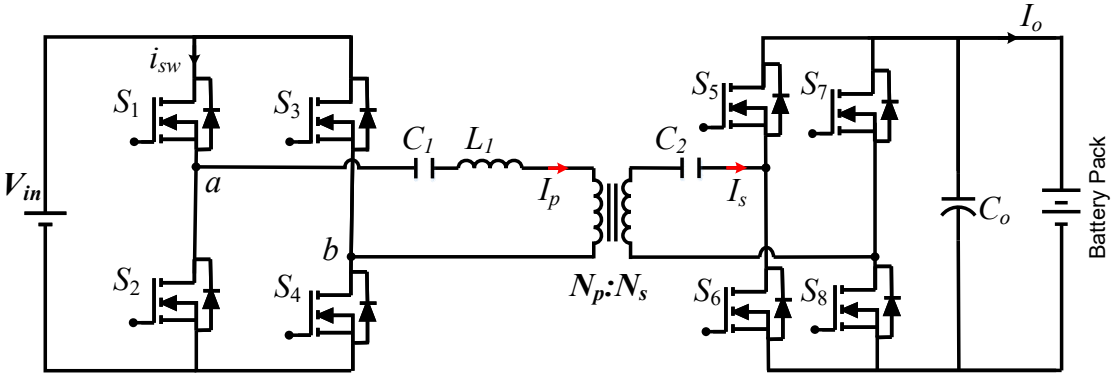

Fig. 4.4 Dual active bridge converter with CLC resonant tank

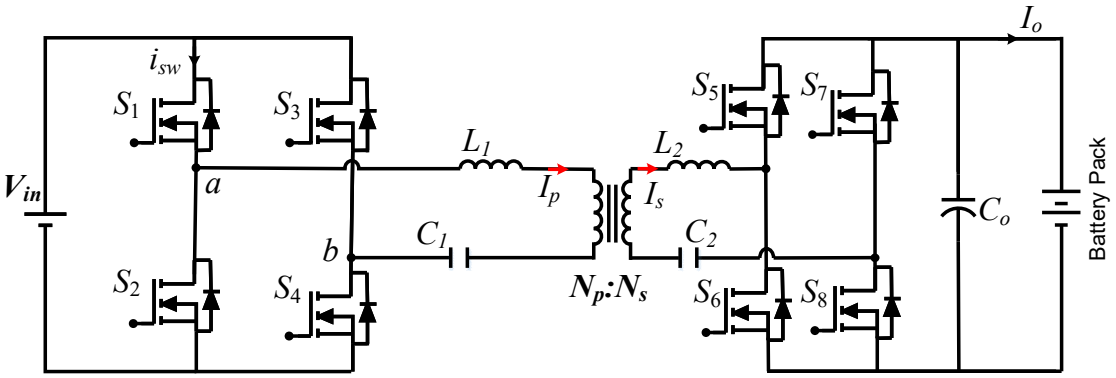

Fig. 4.5 Dual active bridge converter with CLLC resonant tank

4.4 Phase shifted full bridge converter

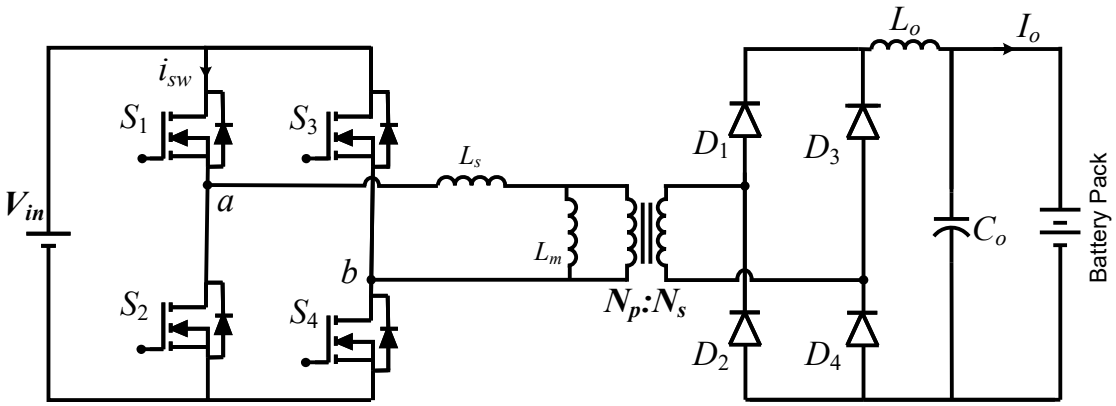

Fig. 4.6 Phase shifted full bridge converter

4.5 PI Controller Tuning with Full Bridge LLC Resonant Converter

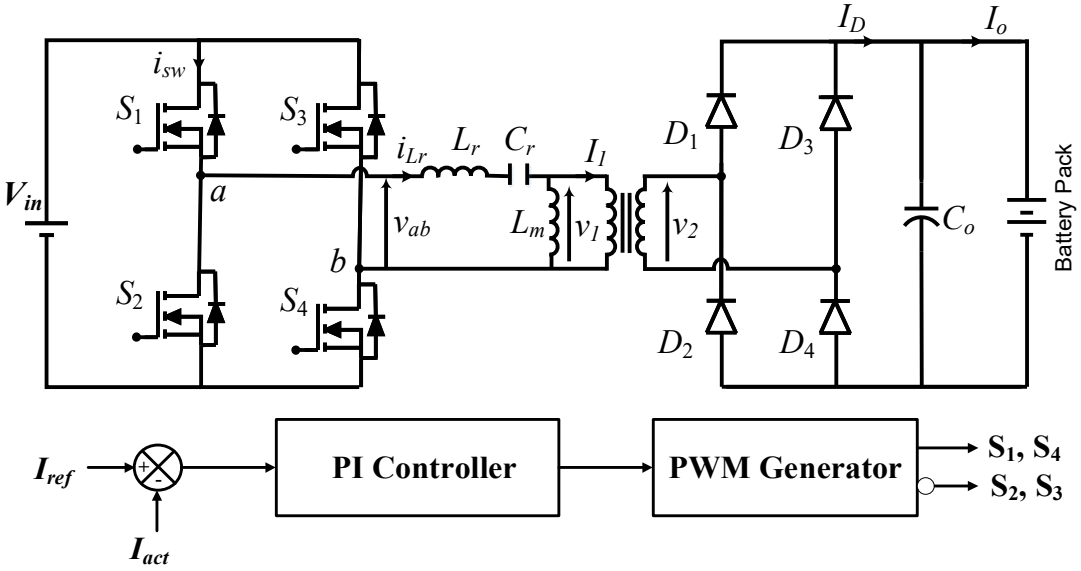

Fig. 4.7 LLC resonant converter with rechargable battery

PI Controller: The PI controller mainly consists of function values of proportional and integral values The PI controller which is implemented for constant current charging is represented by the following equation that represents the proportional and integral values of the function $u(t)$. The error signal is achieved by difference of output signal and reference signal for the converter. The error signal is directly fed back to the system to stabilize the output at constant value. This makes the converter stable and provide a constant current or constant voltage operation [41].

The function $u(t)$ is represented by controlling signal and $e(t)$ is represented by error signal. The controlling signal is defined as the combination of proportional and integral parameters of the converter. P-term and I-term are all contributing to rectify the error output. The P-term is proportional to the error signal, the I-term is the integral to the error signal. The parameters of the controller are represented by proportional gain K_p, integral gain K_i.

$$u(t) = k\left[e(t) + \frac{1}{T_i}\int_0^t e(T)dT \right] \tag{4.1}$$

where, T_i stands for integral time of the specified design of PI controller. The integral parameter of (4.1) represents previous value of errors and the proportional function estimates error corresponding to present value. All these values indicate best optimization of error signal which is generated by comparing the actual and standard signal. Thus, parameters of proportional and integral are quite important to tune PI controller after number of iterations [42].

This term "current error (I_e)" refers to the discrepancy between a real current value and its standard current value of converter. The resulting current error (I_e) signal is passed to PI controller that standardize the value of current for constant charging. Thus, it is important to check the error signal of current at each iteration that defines the accuracy of standardization method. Mathematically, it can be represented as follows:

$$d(x) = d(x-1) + G_{pi}\left\{ I_e(x) - I_e(x-1) \right\} + G_{ii} I_e(x) \tag{4.2}$$

where G_{pi} represents proportional gain and G_{ii} represents integral gain of the PI controller for constant charging.

PWM and a voltage controller are used, which is utilized by the standard LLC resonant converter. The PI controller processes the voltage error (V_{oe}) that is produced by comparing the given reference output voltage and standard battery voltage [43]. The iteration is executed till values near to the standard values is achieved. As it approaches to the standard values, the iterations are stopped and mark the values of PI tuning. The output is expressed as follows:

$$f(x) = f(x-1) + G_{pg}\{V_{oe}(x) - V_{oe}(x-1\} + G_{ig}V_{oe}(x) \quad (4.3)$$

Where G_{pg} represents proportional gain value and G_{ig} represents integral gain of the given converter.

Equations (4.1), (4.2), and (4.3) help to define the values of proportional and integral of the converter. The closed loop converter helps to stabilize the output values to a desired value which is further implemented to obtain charging conditions [44][45].

The optimal charging is achieved by fine tuning of PI Controller. The closed loop converter helps to stabilize the output values to a desired value which is further implemented to obtain charging conditions. PWM and a voltage controller are used, which is utilized by the standard LLC resonant converter.

The PI controller processes the voltage error (V_{oe}) that is produced by comparing the given reference output voltage and standard battery voltage. The iteration is executed till values near to the standard values is achieved. As it approaches to the standard values, the iterations are stopped and mark the values of PI tuning. All these values indicate best optimization of error signal which is generated by comparing the actual and standard signal.

CHAPTER 5

LLC RESONANT CONVERTER WITH EV CHARGING

5.1 Charging methodology:

There are mainly two ways to charge a battery: constant voltage, constant current charging methods. Both charging methods are employed based on the requirement and application.

A. Constant current charging method: The value of current remains constant while charging the battery. The level of current signal is considered at approximately 9.85% of the maximum rating of battery during charging the batteries at constant value of current [50]. The main drawback of long duration of charging is that as the battery is overcharged due to constant current charging, it may increase the temperature of battery which further overheats and require instant replacement of battery. This constant current charging technique is executed with lithium ion and lead acid type of batteries [48].

B. Constant voltage charging method: In order to avoid overcharging, battery may also charged at constant voltage. The power supply maintains a constant voltage as long as, the charger provides a complete path to flow the full value of current through the battery [47][48]. The value of current begins to decrease to the least min value of threshold voltage that is attained by the converter. Lead acid batteries can be charged quickly with this methodology [50].

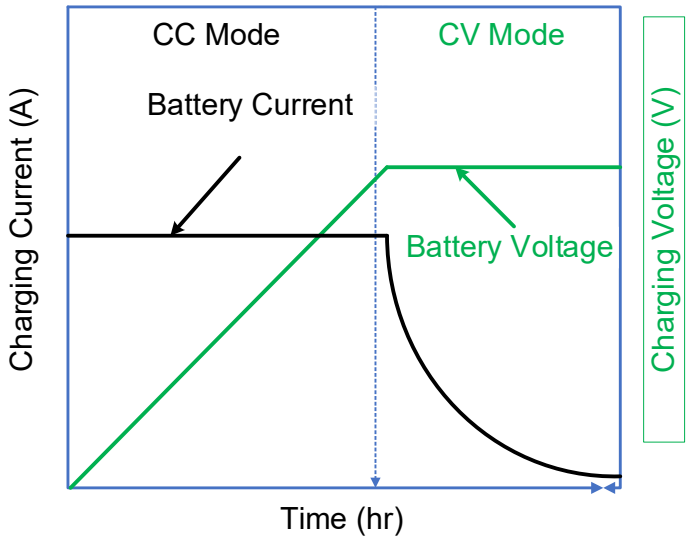

Fig. 5.1 Charging methodolgy representing Constant current and constant voltage

5.2 Design flow of converter:

The proper values of gain are obtained by selecting the nominal voltage, min nominal voltage and max nominal voltage of the converter specifications. The values of resonant tank circuit are calculated by selecting quality factor (Q_{max}) and gain (m) value. By selecting the Q_{max} value of 0.4 and m = 6.3 for designed converter design.

The design of the converter is followed by these following steps:

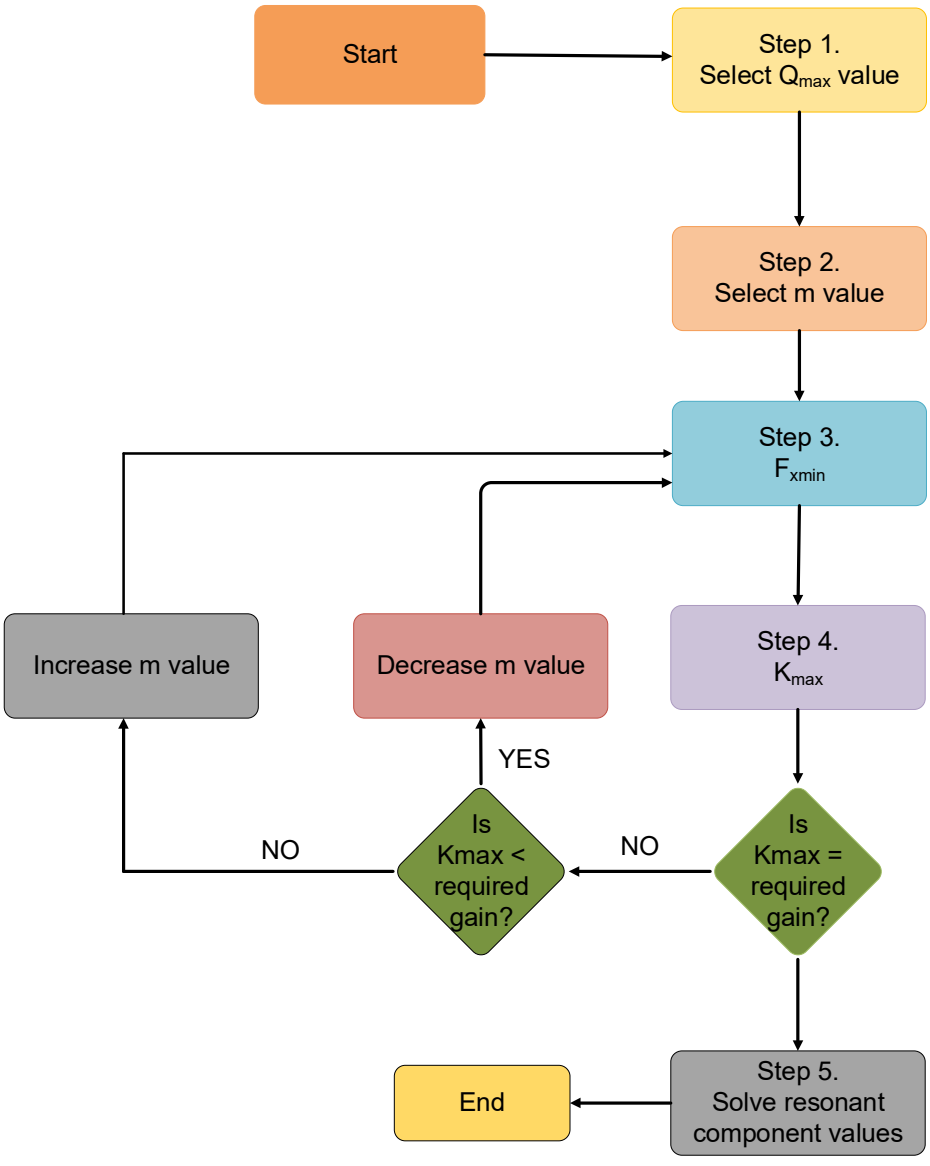

Fig 5.2 Designing steps of converter

Due to iterative steps of gain, its region of operation is defined and operated at specific value. The gain and frequency of converter defines the range of operation that is mentioned in Chapter (3). The converter is designed to operate in inductive region to achieve ZVS condition [51]. The transfer function of the converter is represented by Eq (5.1) and mentioned in Chapter (3)

$$\frac{V_{o1}}{V_{in1}} = \frac{(8/\pi^2)\omega_x^{\,2}}{\sqrt{(\omega_x^{\,2} + (\frac{L_r}{L_m}(\omega_x^{\,2}-1))^2 + Q^2\omega_x^{\,2}(\omega_x^{\,2}-1)^2}} \tag{5.1}$$

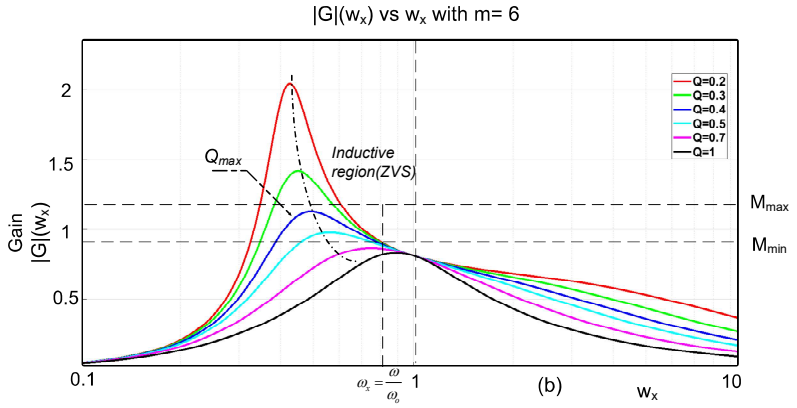

Fig 5.3. Gain versus frequency curve of resonant converter at *m = 6.3, Q = 0.4*

LLC resonant converter of 1500 watts is designed and modelled with MATLAB/SIMULINK software for output voltage rating of 96 V and constant current of 15.625 A. The converter is used for charging of Li-ion battery for constant current mode with initial state of charge of 45%. The system parameters are presented by Table I. mentioned in Chapter 2

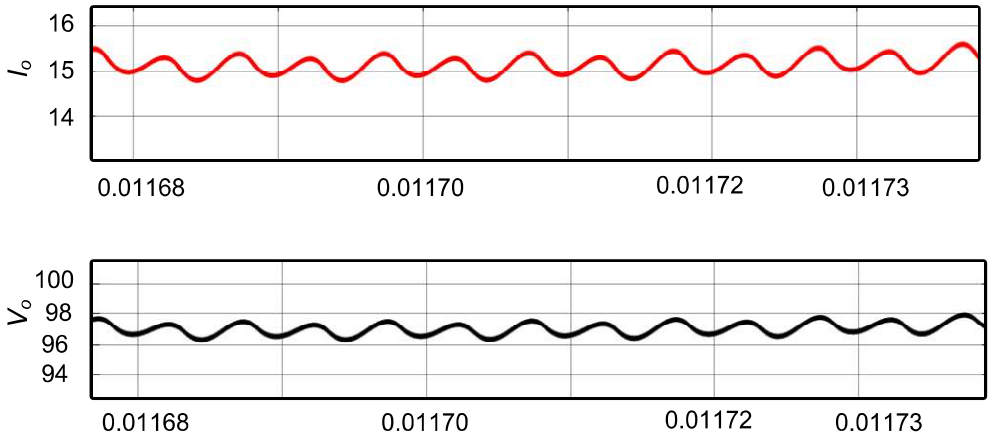

Fig. 5.4. Output current, output voltage

The output current and voltage at LLC resonant converter is represented by Fig 5.4. The ripple in the output voltage and output current are minimum which is suitable for battery charging application. This model can be applied in EV level 1 charger (upto 3.3kW) and upon extending the rating of converter can be applied in level 2 and level 3 chargers

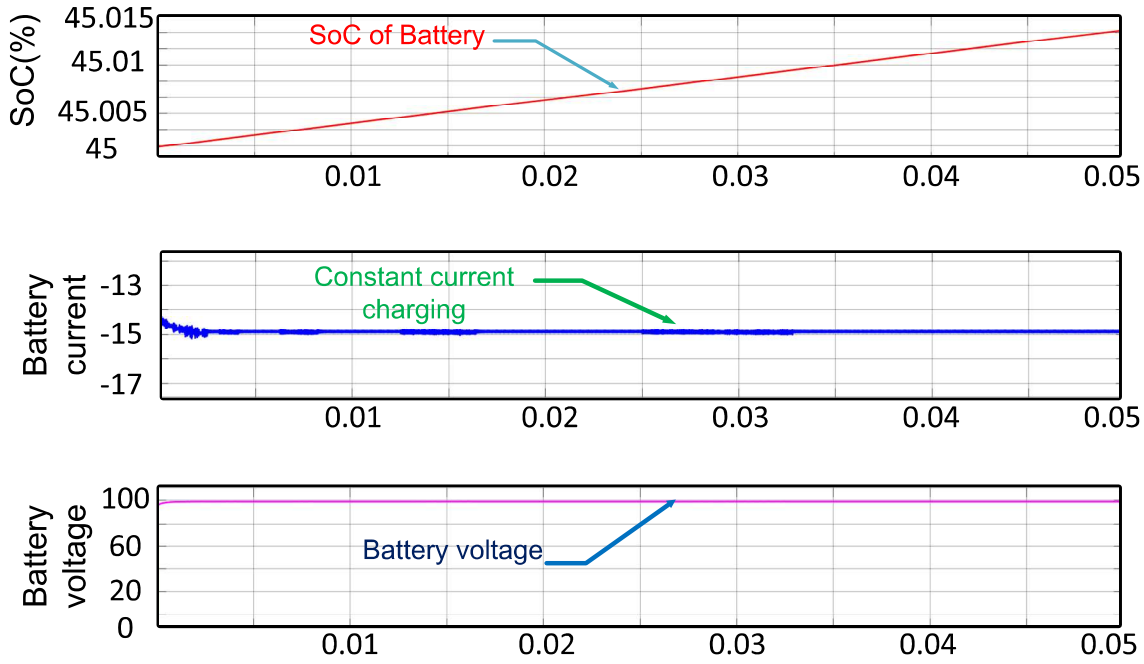

Fig. 5.5. SoC (%), Constant Charging Current, Battery Voltage.

The SoC of battery is represented by Fig. 5.5 which shows the charging case of the converter by the linearly increasing graph. The constant negative value of current represents behavior of constant current charging method. Battery voltage and current values are maintained at constant level of 96 volts and 15.625 A. This defines the constant current and constant voltage charging for level 1.

Zero voltage switching behavior is also achieved by switching the MOSFET voltage and current at a particular instant of time. The switching is performed to maintain the losses at their minimum level at such high frequency operation and provides soft switching to the converter. This switching current is obtained through S_2, S_3 switches and the same action is achieved with S_1, S_4 switches during next cycle of gating pulse of converter as mentioned in Fig 4.9.

The zero-voltage switching is obtained to mitigate the switching losses and improves the efficiency of converter for the application of EV charging.

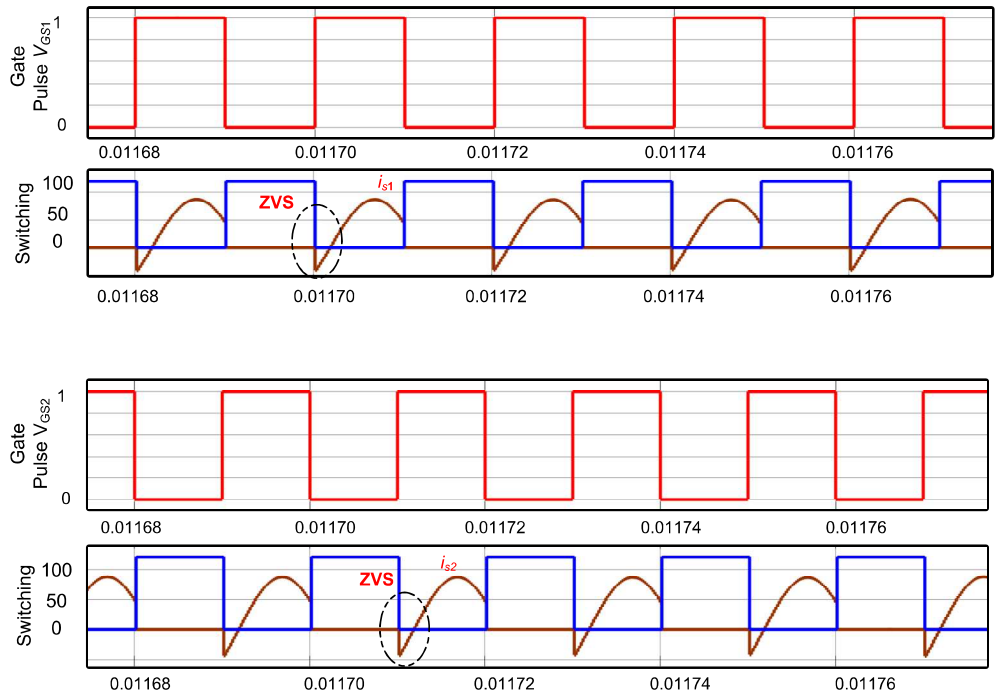

Fig. 5.6. Gate Pulse, Switch voltage and Switch current across MOSFET representing ZVS

5.3 Transformer Behavior During EV Battery Charing

A high frequency transformer is used as it light in weight and comparatively small in size and can be implemented in the level 1 charging. Not just it transforms the input voltage and input current but also provides galvanic isolation. Fig 5.7 represents the voltage and current at the primary and secondary side of transformer during Battery Charging.

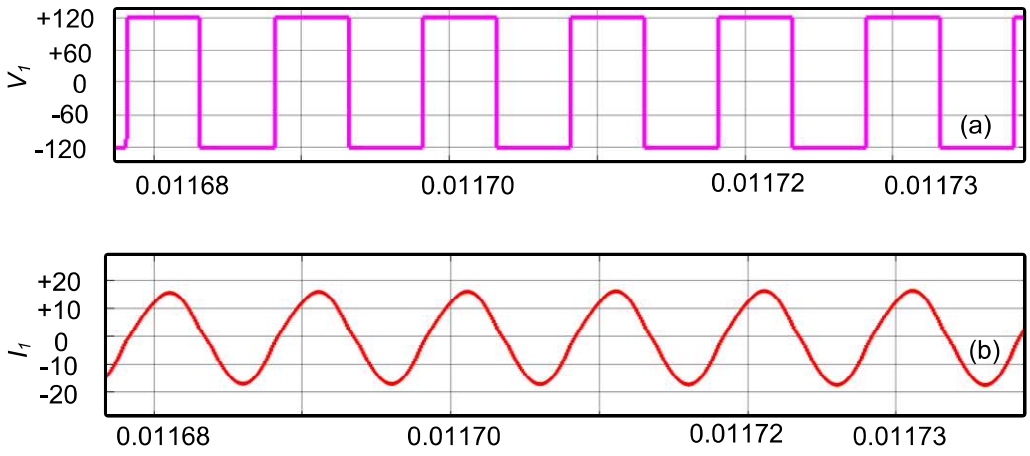

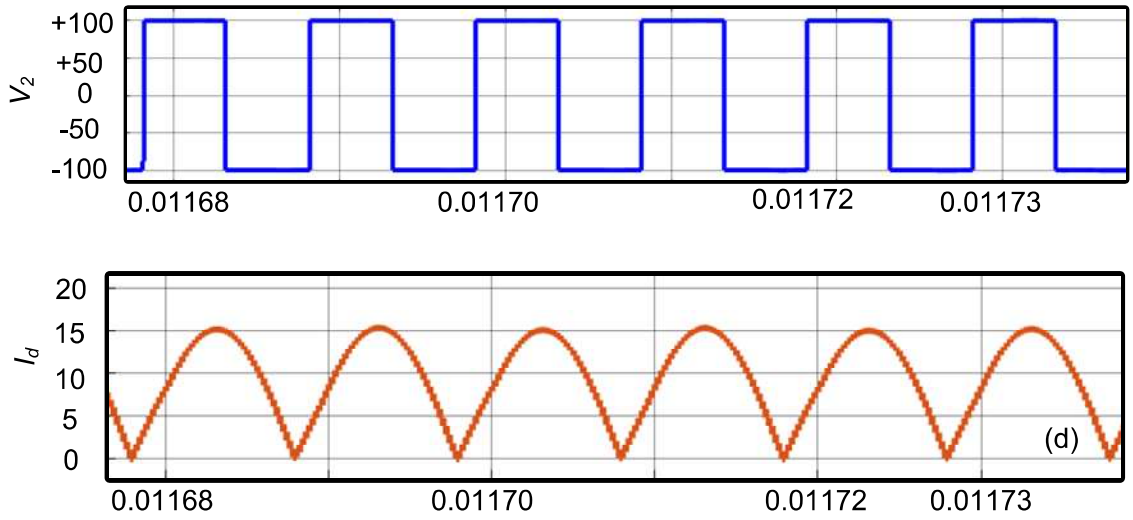

Fig. 5.7. (a), (b) Input voltage and current at primary side, and (c), (d) secondary side voltage and current I_d.

CHAPTER 6

CONCLUSION AND FUTURE WORK

6.1 Work Summary

Resonant converter is implemented for EV charging applications and simulated using MATLAB Simulink environment. The converter is evaluated and operated under various frequencies to get the desired results. This allows us to operate the converter in different application of charging [52]. It is analyzed that the LLC resonant converter always provides efficient and better performance at the frequency where resonance is achieved. Furthermore, a Full-Bridge LLC resonant converter is integrated with PI controller at it has been obtained that it provides constant current applications. To reduce the effect of significant amount of current flowing at the switching, Full-bridge LLC resonant converter with high value of magnetizing inductance is designed. The presence of inductance present in magnetizing branch of converter suppresses effect of inrush current which can be utilized in various EV charging topologies [55].

It has been also observed that the Full Bridge LLC resonant converter design operates at multiple level of voltages that performs at 110 V_{rms} – 230$V_{rms.}$ This closed loop topology can be applied to various converters having power rating of 1.5kW to 5 kW. Battery is charged at the charging current of value 15.625 A and battery voltage of 96 volts. This constant current charging method avoids the overheating problem. PI controller is tuned properly using closed loop configuration for the high switching operation and better efficiency.

6.2 Future Work

This model can be applied in EV level 1 charger (upto 3.3kW) and upon extending the rating of converter can be applied in level 2 and level 3 charger with proper hardware prototype and minimal number of ripples present in the output voltage and current values.

REFRENCES

[1] M. Kesler, M. Kisacikoglu, and L. Tolbert, "Vehicle-to-Grid Reactive Power Operation Using Plug-in EV Bidirectional Off-Board Charger," IEEE Transactions on Industrial Electronics, vol. PP, pp. 1-1, 2014.

[2] J. C. Mukherjee and A. Gupta, "A Review of Charge Scheduling of EVs in Smart Grid," IEEE Systems Journal, vol. 9, pp. 1541-1553, 2015

[3] C. C. Chan, "An overview of EV technology," Proceedings of the IEEE, vol. 81, pp. 1202-1213, 1993.

[4] Z. Xiaohu, S. Lukic, S. Bhattacharya, and A. Huang, "Design and control of grid-connected converter in bi-directional battery charger for Plug-in hybrid EV application," in Vehicle Power and Propulsion Conference, 2009. VPPC '09. IEEE, 2009, pp. 1716-1721.

[5] Y. Ota, H. Taniguchi, T. Nakajima, K. M. Liyanage, J. Baba, and A. Yokoyama, "Autonomous Distributed V2G (Vehicle-to-Grid) Satisfying Scheduled Charging," IEEE Transactions on Smart Grid, vol. 3, pp. 559-564, 2012.

[6] U. K. Madawala and D. J. Thrimawithana, "A Bidirectional Inductive Power Interface for EVs in V2G Systems," IEEE Transactions on Industrial Electronics, vol. 58, pp. 4789-4796, 2011.

[7] H. Liu, Z. Hu, Y. Song, and J. Lin, "Decentralized Vehicle-to-Grid Control for Primary Frequency Regulation Considering Charging Demands," IEEE Transactions on Power Systems, vol. 28, pp. 3480-3489, 2013.

[8] M. Yilmaz and P. T. Krein, "Review of the Impact of Vehicle-to-Grid Technologies on Distribution Systems and Utility Interfaces," IEEE Transactions on Power Electronics, vol. 28, pp. 5673-5689, 2013.

[9] M. Yilmaz and P. T. Krein, "Review of Battery Charger Topologies, Charging Power Levels, and Infrastructure for Plug-In Electric and Hybrid Vehicles," IEEE Transactions on Power Electronics, vol. 28, pp. 2151-2169, 2013.

[10] A. Westgeest and L. Brett, "Improving safety and performance testing for EV batteries," in 2013 World EV Symposium and Exhibition (EVS27), 2013, pp. 1-4.

[11] P. A. Cassani and S. S. Williamson, "Significance of Battery Cell Equalization and Monitoring for Practical Commercialization of Plug-In Hybrid Electric

Vehicles," in 2009 Twenty-Fourth Annual IEEE Applied Power Electronics Conference and Exposition, 2009, pp. 465-471.

[12] A. Khaligh and Z. Li, "Battery, Ultracapacitor, Fuel Cell, and Hybrid Energy Storage Systems for Electric, Hybrid Electric, Fuel Cell, and Plug-In Hybrid EVs: State of the Art," IEEE Transactions on Vehicular Technology, vol. 59, pp. 2806-2814, 2010.

[13] P. Ramadass, B. Haran, R. White, and B. N. Popov, "Performance study of commercial LiCoO2 and spinel-based Li-ion cells," Journal of Power Sources, vol. 111, pp. 210-220, 9/23/ 2002.

[14] K. Nihal, "Rechargeable batteries and battery management systems design," in IECON 2010 - 36th Annual Conference on IEEE Industrial Electronics Society, 2010, pp. 1-2.

[15] J. T. Salihi, P. D. Agarwal, and G. J. Spix, "Induction Motor Control Scheme for Battery-Powered Electric Car (GM-Electrovair I)," IEEE Transactions on Industry and General Applications, vol. IGA-3, pp. 463-469, 1967.

[16] S. Jurkovic, K. M. Rahman, and P. J. Savagian, "Design, optimization and development of electric machine for traction application in GM battery EV," in 2015 IEEE International Electric Machines & Drives Conference (IEMDC), 2015, pp. 1814-1819.

[17] P. Leijen and N. Kularatna, "Developing a monitoring system for Toyota Prius battery-packs for longer term performance issues," in 2013 IEEE International Symposium on Industrial Electronics, 2013, pp. 1-6.

[18] K. J. Kelly, M. Mihalic, and M. Zolot, "Battery usage and thermal performance of the Toyota Prius and Honda Insight during chassis dynamometer testing," in Seventeenth Annual Battery Conference on Applications and Advances. Proceedings of Conference (Cat. No.02TH8576), 2002, pp. 247-252.

[19] W. Renhart, C. Magele, and B. Schweighofer, "FEM-Based Thermal Analysis of NiMH Batteries for Hybrid Vehicles," IEEE Transactions on Magnetics, vol. 44, pp. 802-805, 2008.

[20] A. Hoke, A. Brissette, K. Smith, A. Pratt, and D. Maksimovic, "Accounting for Lithium-Ion Battery Degradation in EV Charging Optimization," IEEE Journal of Emerging and Selected Topics in Power Electronics, vol. 2, pp. 691-700, 2014

[21] J. R. M. D. Reyes, R. V. Parsons, and R. Hoemsen, "Winter Happens: The Effect of Ambient Temperature on the Travel Range of EVs," IEEE Transactions on Vehicular Technology, vol. 65, pp. 4016-4022, 2016.

[22] O. Tremblay, L. A. Dessaint, and A. I. Dekkiche, "A Generic Battery Model for the Dynamic Simulation of Hybrid EVs," in 2007 IEEE Vehicle Power and Propulsion Conference, 2007, pp. 284-289.

[23] H. He, R. Xiong, X. Zhang, F. Sun, and J. Fan, "State-of-Charge Estimation of the Lithium-Ion Battery Using an Adaptive Extended Kalman Filter Based on an Improved Thevenin Model," IEEE Transactions on Vehicular Technology, vol. 60, pp. 1461-1469, 2011.

[24] H. S. Park, C. E. Kim, C. H. Kim, G. W. Moon, and J. H. Lee, "A Modularized Charge Equalizer for an HEV Lithium-Ion Battery String," IEEE Transactions on Industrial Electronics, vol. 56, pp. 1464-1476, 2009.

[25] A. Affanni, A. Bellini, G. Franceschini, P. Guglielmi, and C. Tassoni, "Battery choice and management for new-generation EVs," IEEE Transactions on Industrial Electronics, vol. 52, pp. 1343-1349, 2005.

[26] S. Dey, B. Ayalew, and P. Pisu, "Combined estimation of State-of-Charge and State-of-Health of Li-ion battery cells using SMO on electrochemical model," in 2014 13th International Workshop on Variable Structure Systems (VSS), 2014, pp. 1-6.

[27] R. Milligan, T. Muneer, and I. Smith, "A comparative range approach using the Real-world Drive Cycles and the Battery EV," in 2015 IEEE International Transportation Electrification Conference (ITEC), 2015, pp. 1-5.

[28] Y. Attia, A. Abdelrahman, M. Hamouda, and M. Youssef, "SiC devices performance overview in EV DC/DC converter: A case study in a Nissan Leaf," in 2016 IEEE Transportation Electrification Conference and Expo, Asia-Pacific (ITEC Asia-Pacific), 2016, pp. 214-219.

[29] W. Liangrong, L. Jianing, X. Guoqing, X. Kun, and S. Zhibin, "A novel battery charger for plugin hybrid EVs," in Information and Automation (ICIA), 2012 International Conference on, 2012, pp. 168-173.

[30] S. R. Osman, N. A. Rahim, and S. Jeyraj, "Single current sensor with multiple constant current charging method in solar battery charger," in 3rd IET International Conference on Clean Energy and Technology (CEAT) 2014, 2014, pp. 1-5.

[31] Y. D. Lee and S. Y. Park, "Rapid charging strategy in the constant voltage mode for a high-power Li-Ion battery," in 2013 IEEE Energy Conversion Congress and Exposition, 2013, pp. 4725-473

[32] S. Li, C. Zhang, and S. Xie, "Research on Fast Charge Method for Lead-Acid EV Batteries," in Intelligent Systems and Applications, 2009. ISA 2009. International Workshop on, 2009, pp. 1-5.

[33] S. G. Abeyratne, P. S. N. Perera, H. S. Jayakody, S. M. K. B. Samarakoon, and R. R. S. De Bulathge, "Soft Switching fast charger for batteries used in Renewable Energy applications and EVs," in Industrial and Information Systems (ICIIS), 2012 7th IEEE International Conference on, 2012, pp. 1-6.

[34] M. Chen and G. A. Rincon-Mora, "Accurate, Compact, and Power-Efficient Li-Ion Battery Charger Circuit," IEEE Transactions on Circuits and Systems II: Express Briefs, vol. 53, pp. 1180- 1184, 2006.

[35] L. Yi-Hwa, T. Jen-Hao, and L. Yu-Chung, "Search for an optimal rapidcharging pattern for lithium-ion batteries using ant colony system algorithm," IEEE Transactions on Industrial Electronics, vol. 52, pp. 1328-1336, 2005.

[36] S. A. Singh and S. S. Williamson, "Comprehensive review of PV/EV/grid integration power electronic converter topologies for DC charging applications," in 2014 IEEE Transportation Electrification Conference and Expo (ITEC), 2014, pp. 1-5.

[37] S. S. Williamson, A. K. Rathore, and F. Musavi, "Industrial Electronics for Electric Transportation: Current State-of-the-Art and Future Challenges," IEEE Transactions on Industrial Electronics, vol. 62, pp. 3021-3032, 2015.

[38] A. Dubey and S. Santoso, "EV Charging on Residential Distribution Systems: Impacts and Mitigations," IEEE Access, vol. 3, pp. 1871-1893, 2015.

[39] S. Chalia, A. K. Seth and M. Singh, "EV Charging Standards in India and Safety Consideration," 2021 IEEE 8th Uttar Pradesh Section International Conference on Electrical, Electronics and Computer Engineering(UPCON), 2021, pp. 1-6.

[40] T. Kang, C. Kim, Y. Suh, H. Park, B. Kang, and D. Kim, "A design and control of bi-directional non-isolated DC-DC converter for rapid EV

charging system," in 2012 IEEE International Conference on Information and Automation, 2012, pp. 14-21.

[41] International Organization for Standardization (ISO). ISO 6469-3:2011 Electrically propelled road vehicles -- Safety specifications -- Part 3: Protection of persons against electric shock Available:

[42] UL. (2016, 10 December). UL 2231-1 Standard for Safety for Personnel Protection Systems for EV (EV) Supply Circuits: General Requirements. Available:

[43] S. Y. Kim, H. S. Song, and K. Nam, "Idling Port Isolation Control of Three-Port Bidirectional Converter for EVs," IEEE Transactions on Power Electronics, vol. 27, pp. 2495-2506, 2012.

[44] S. Pala and S. P. Singh, "Design, modeling and implementation of Bi-directional buck and boost converter," in 2012 IEEE 5th India International Conference on Power Electronics (IICPE), 2012, pp. 1-6.

[45] A. Nasiri, Z. Nie, S. B. Bekiarov, and A. Emadi, "An On-Line UPS System With Power Factor Correction and Electric Isolation Using BIFRED Converter," IEEE Transactions on Industrial Electronics, vol. 55, pp. 722-730, 2008.

[46] G. Oggier, G. O. García, and A. R. Oliva, "Modulation Strategy to Operate the Dual Active Bridge DC-DC Converter Under Soft Switching in the Whole Operating Range," IEEE Transactions on Power Electronics, vol. 26, pp. 1228-1236, 2011.

[47] M. N. Kheraluwala, R. W. Gascoigne, D. M. Divan, and E. D. Baumann, "Performance characterization of a high-power dual active bridge," IEEE Transactions on Industry Applications, vol. 28, pp. 1294-1301, 1992.

[48] G. G. Oggier, G. O. GarcÍa, and A. R. Oliva, "Switching Control Strategy to Minimize Dual Active Bridge Converter Losses," IEEE Transactions on Power Electronics, vol. 24, pp. 1826-1838, 2009.

[49] M. H. Ryu, H. S. Kim, J. W. Baek, H. G. Kim, and J. H. Jung, "Effective Test Bed of 380-V DC Distribution System Using Isolated Power Converters," IEEE Transactions on Industrial Electronics, vol. 62, pp. 4525-4536, 2015.

[50] T. Jiang, X. Chen, J. Zhang, and Y. Wang, "Bidirectional LLC resonant converter for energy storage applications," in 2013 Twenty-Eighth Annual IEEE Applied Power Electronics Conference and Exposition (APEC), 2013, pp. 1145-1151.

[51] X. Xie, Z. Zhao, C. Zhao, J. M. Zhang, and Z. Qian, "Analysis and Optimization of LLC Resonant Converter With a Novel Over-Current Protection Circuit," IEEE Transactions on Power Electronics, vol. 22, pp. 435-443, 2007.

[52] R. Liu and C. Q. Lee, "The LLC-type series resonant converter-variable switching frequency control," in Proceedings of the 32nd Midwest Symposium on Circuits and Systems, 1989, pp. 509- 512 vol.1.

[53] K. Siri and C. Q. Lee, "Constant switching frequency LLC-type series resonant converter," in Circuits and Systems, 1989., Proceedings of the 32nd Midwest Symposium on, 1989, pp. 513-516 vol.1.

[54] C. J and W. A. F., "Analytic solutions for LLCC parallel resonant converter simplify use of two and three-element converters," IEEE Transactions on Power Electronics, vol. 13, pp. 235-243, 1998.

[55] G. Y, L. Z, and Q. Z, "Three level LLC series resonant DC/DC converter," in 2004 Nineteenth Annual IEEE Applied Power Electronics Conference and Exposition (APEC), 2004, pp. 1647- 1652 Vol.3.

[56] B. Yang, F. C. Lee, A. J. Zhang, and H. Guisong, "LLC resonant converter for front end DC/DC conversion," in Applied Power Electronics Conference and Exposition, 2002. APEC 2002. Seventeenth Annual IEEE, 2002, pp. 1108-1112 vol.2.

[57] C. Gould, C. M. Bingham, D. A. Stone, and M. P. Foster, "CLL resonant converters with output short-circuit protection," Electric Power Applications, IEE Proceedings -, vol. 152, pp. 1296-1306, 2005.

[58] C. Gould, D. A. Stone, M. P. Foster, and C. Bingham, "State-variable modelling of CLL resonant converters," in Second International Conference on Power Electronics, Machines and Drives (PEMD 2004). 2004, pp. 214-219 Vol.1.

[59] C. H. Chang, C. Hung-Liang, C. En-Chih, C. Chun-An, and C. Hung-Yi, "Modeling and design of the LLC resonant converter used in solar array simulator," in 2012 7th IEEE Conference on Industrial Electronics and Applications (ICIEA), 2012, pp. 653-658.

[60] G. Pledl, M. Tauer, and D. Buecherl, "Theory of operation, design procedure and simulation of a bidirectional LLC resonant converter for vehicular applications," in 2010 IEEE Vehicle Power and Propulsion Conference, 2010, pp. 1-5.

PUBLICATION

1. Shreyas, Mayank Kumar, "Design and Analysis of LLC Resonant Converter for Electric Vehicle Battery Charging" in 2023 IEEE 3rd International Conference on Sustainable Energy and Future Electric Transportation (IEEE SEFET 2023) – **(Accepted)**